

# Resolution Effects in the Hybrid Strong/Weak Coupling Model

---

Zachary Hulcher,<sup>a</sup> Daniel Pablos,<sup>b</sup> Krishna Rajagopal<sup>a</sup>

<sup>a</sup>*Center for Theoretical Physics, Massachusetts Institute of Technology, Cambridge, MA 02139 USA*

<sup>b</sup>*Department of Physics, McGill University, 3600 University Street, Montréal, QC, H3A 2T8, Canada*

*E-mail:* [zhulcher@mit.edu](mailto:zhulcher@mit.edu), [pablosd@physics.mcgill.ca](mailto:pablosd@physics.mcgill.ca),  
[krishna@mit.edu](mailto:krishna@mit.edu)

ABSTRACT:

Within the context of a hybrid strong/weak coupling model of jet quenching, we study the consequences of the fact that the plasma produced in a heavy ion collision cannot resolve the substructure of a collimated parton shower propagating through it with arbitrarily fine spatial resolution. We introduce a screening length parameter,  $L_{\text{res}}$ , proportional to the inverse of the local temperature in the plasma, estimating a range for the value of the proportionality constant via comparing weakly coupled QCD calculations and holographic calculations appropriate in strongly coupled plasma. We then modify the hybrid model so that when a parton in a jet shower splits, its two offspring are initially treated as unresolved, and are only treated as two separate partons losing energy independently after they are separated by a distance  $L_{\text{res}}$ . This modification delays the quenching of partons with intermediate energy, resulting in the survival of more hadrons in the final state with  $p_T$  in the several GeV range. We analyze the consequences of different choices for the value of the resolution length,  $L_{\text{res}}$ , and demonstrate that introducing a nonzero  $L_{\text{res}}$  results in modifications to the jet shapes and jet fragmentations functions, as it makes it more probable for particles carrying a small fraction of the jet energy at larger angles from the jet axis to survive their passage through the quark-gluon plasma. These effects are, however, small in magnitude, something that we confirm via checking for effects on missing- $p_T$  observables.

---

## Contents

|          |   |           |
|----------|---|-----------|
| <b>1</b> | <b>Introduction</b>   | <b>1</b>  |
| <b>2</b> | <b>Brief Summary of the Hybrid Strong/Weak Coupling Model</b>                   | <b>4</b>  |
| <b>3</b> | <b>The Resolution Length within QGP</b>   | <b>7</b>  |
| <b>4</b> | <b>Implementation of the Effects of Resolution within the Hybrid Model</b>      | <b>9</b>  |
| <b>5</b> | <b>The Effects of Resolution on Jet Observables</b>                             | <b>13</b> |
| 5.1      | Distribution of energy lost by partons in a jet                                 | 13        |
| 5.2      | Jet $R_{AA}$ , including its Dependence on the Jet Reconstruction Parameter $R$ | 15        |
| 5.3      | Fragmentation functions and jet shapes  | 16        |
| 5.4      | Two missing- $p_T$ observables  | 20        |
| <b>6</b> | <b>Discussion and Outlook</b>   | <b>23</b> |

---

## 1 Introduction

High energy heavy ion collisions at the Relativistic Heavy Ion Collider (RHIC) and the Large Hadron Collider (LHC) provide a key window into the dynamics and properties of droplets of the hot matter that filled the microseconds old universe, called quark-gluon plasma (QGP). Experiments at these facilities have demonstrated that in the experimentally accessible range of temperatures, up to several times hotter than the crossover temperature at which cooling QGP becomes ordinary hadronic matter, droplets of QGP exhibit strong collective phenomena [1–7], with the dynamics of the rapid expansion and cooling of the initially lumpy droplets produced in the collisions successfully described by the equations of relativistic viscous hydrodynamics [8–18]. The ratio of the shear viscosity,  $\eta$ , to the entropy density,  $s$ , serves as a benchmark, because in a weakly coupled plasma,  $\eta/s \propto 1/g^4$  (with  $g$  the gauge coupling), meaning that this ratio is large, whereas  $\eta/s = 1/4\pi$  in the high temperature phase (conventionally called the plasma phase even though in reality it is a liquid) of any gauge theory that has a dual gravitational description in the limit of strong coupling and large number of colors [19–21]. Comparisons between hydrodynamic calculations of, and experimental measurements of, anisotropic flow in heavy ion collisions indicate that the QGP in QCD has an  $\eta/s$  that is comparable to, and in particular not much larger than  $1/4\pi$ , meaning that QGP itself is a strongly coupled liquid.

The discovery that QGP is a strongly coupled liquid challenges us to find experimental means to probe its structure and properties. The only probes that we have available are those produced in the same heavy ion collisions in which the droplets of QGP themselves are produced. Here we shall focus entirely on the use of high transverse momentum jets, produced at the moment of the

collision in initial hard scatterings, as probes. As a partonic jet shower propagates through the strongly coupled plasma created in a heavy ion collision, the partons lose energy and momentum as a consequence of their strong interactions with the plasma, creating a wake in the plasma. These interactions lead to a reduction in the jet energy (or quenching) and to modifications of the properties of jets produced in heavy ion collisions relative to those of their counterparts produced in proton-proton collisions, that propagate in vacuum. By pursuing a large suite of jet measurements, the different LHC collaborations have observed strong modification of different jet observables in heavy ion collisions [22–47], making jets promising probes for medium diagnostics. The first experimental constraints on jet quenching came from hadronic measurements at RHIC [48–50]. Analyses of jets themselves and their modification are also being performed at RHIC [51–56] and are one of the principal scientific goals of the planned sPHENIX detector [57].

A complete theoretical description of the processes by which jets are modified via passage through QGP remains challenging, because it is a multi-scale problem. On the one hand, the production of jets and the processes via which an initial hard parton fragments into a shower are weakly coupled hard processes. On the other hand, the interaction of jets with the medium, the dynamics of softer components within jets, and the dynamics of the wake produced in the medium by the jets are all sensitive to strongly coupled dynamics of the plasma at scales of order its temperature. One class of approaches is based upon assuming that resummed weakly coupled analyses can be applied almost throughout. (See Refs. [58–63] for reviews and Refs. [64–71] for Monte Carlo tools for analyzing jet observables that are being developed based upon these approaches.) However, the observation that QGP is a strongly coupled liquid tells us that physics at scales of order its temperature is governed by strong coupling dynamics. This realization has led to many fruitful connections between the physics of the QCD plasma and the gauge/gravity duality [72]. This technique allows us rigorous and quantitative access to nonperturbative, strongly coupled, physics in a large family of non-abelian gauge theory plasmas that have a dual holographic description in terms of a black hole spacetime in a gravitational theory with one higher dimension. Although the current formulation of the duality has not been shown to apply to QCD, the study of the plasmas in gauge theories that do have a holographic description has led to many insights into the dynamics of hot deconfined matter in QCD. (See Refs. [73–75] for reviews.) Within this context, there have been many interesting studies that address varied aspects of the interaction between high energy probes and strongly coupled plasma [76–110]. None of these approaches, however, can treat the intrinsically weakly coupled processes of jet production and fragmentation, since in all examples that are currently accessible via gauge/gravity duality the gauge theory is strongly coupled in the ultraviolet, rather than asymptotically free.

To address the multi-scale dynamics of QCD jets in strongly coupled plasma more fully, in Refs. [111–113] two of us together with coauthors have introduced and developed a phenomenological hybrid strong/weak coupling approach to analyzing jet quenching. In this approach, different physical processes of relevance for the interaction of developing jet showers with the quark gluon plasma are treated differently: the production and evolution of the jet shower is treated perturbatively, because the physics governing these processes is expected to be weakly coupled, while the interaction between each of the partons formed in the shower with the medium is assumed to follow the rate of energy loss of an energetic quark in strongly coupled plasma obtained via holographic calculations in Refs. [105, 107].

In this paper we remedy a lacuna in the hybrid model of Refs. [111–113]. In the model as developed to now, when a parton in the jet shower splits, the two resulting offspring partons are treated as if they separately and independently lose energy to the plasma from the moment of the splitting. This cannot be correct: when the two offspring are separated by a distance that is  $\ll 1/T$ , there is no way that a medium with temperature  $T$  can resolve them and respond to them separately. Our goal in this paper is to assess how important it is to include the finite resolving power of the medium in the hybrid strong/weak coupling model by introducing a simple extension of the model allowing us to treat the two offspring as a single unresolved parton, losing energy as the parent parton was, until the offspring are separated by a distance  $L_{\text{res}}$  that we shall specify. This is certainly an oversimplification, as we shall explain, but it allows us to characterize the consequences of finite resolution via introducing only a single new parameter into the model and calculating its effects on several key observables. We find that introducing a nonzero resolution length,  $L_{\text{res}}$ , brings the predictions of the hybrid model for the jet fragmentation function and the jet shape into slightly better agreement with data, but the effects are small in magnitude. We also check whether these effects are sufficient to bring the model predictions for the so-called missing- $p_T$  observables into agreement with data in the  $p_T$ -range of several GeV where discrepancies have been found [113], and in this case find no significant improvement. This lends indirect support to the alternative explanation suggested in Ref. [113] for these particular discrepancies, namely that the wake created in the liquid medium by a jet does not fully thermalize.

We begin in Section 2 by providing a brief review of the hybrid model of Refs. [111–113]. In Section 3, we then describe the modification to the model that we shall investigate, introducing a resolution length,  $L_{\text{res}}$ , that must be of order the Debye length in the plasma, as we shall discuss. Partons separated by less than  $L_{\text{res}}$  cannot be resolved by the medium and so should lose energy in the hybrid model as one parton (with their combined energy and momentum) does. When two colored partons propagating through the plasma are sufficiently close to each other, this should be physically indistinguishable from a single parton with the same total energy, momentum, and color charge propagating through the same plasma. Analogous observations have been made in at least two other contexts: in weakly coupled analyses of how QCD dipoles with varying sizes radiate gluons as they propagate through the plasma, where the analogous observation arises as a consequence of quantum interference [114–116], and in an analysis of strongly coupled proxies for pairs of jets in holography [108]. Once partons are separated by more than  $L_{\text{res}}$ , however, they behave in the plasma (and in particular should lose energy) as separate partons. In the hybrid model as developed in Refs. [111–113],  $L_{\text{res}} = 0$ : when a parton splits in two, its offspring start losing energy as if they were independent immediately. In Section 4, we describe our simplified implementation of the effects of resolution,  $L_{\text{res}} \neq 0$ , in the hybrid model. In Section 5, we assess the consequences of introducing a nonzero  $L_{\text{res}}$  for several observables calculated previously in the hybrid model, namely hadronic jet shapes, hadronic fragmentation functions, and two different missing- $p_T$  observables. Introducing resolution effects means that partons in the shower that have a relatively low energy “hide” for a while, since as far as the plasma is concerned they remain lumped together with their higher energy parent parton for a longer time. This makes it less likely that they lose all their energy to the medium and more likely that they survive as components of the jet until the jet hadronizes. This results in small modifications to both the fragmentation function (enhancing it for hadrons carrying a modest fraction of the jet energy) and the jet shape (enhancing

it at moderate angles, where these hadrons are found). We close in Section 6 with a discussion and a look ahead.

## 2 Brief Summary of the Hybrid Strong/Weak Coupling Model

The hybrid strong/weak coupling model is a phenomenological approach to the multi-scale problem one encounters in describing jet quenching phenomena in heavy-ion collisions. The production of high energy jets is under good theoretical control through perturbative QCD calculations due to the high virtuality scale which characterizes the process; furthermore, these processes occur at very early time scales, much earlier than the formation of the QGP. This high virtuality relaxes by successive splittings, which are again well described in perturbative QCD, via DGLAP (Dokshitzer-Gribov-Lipatov-Altarelli-Parisi) evolution. Indeed, the medium temperature  $T$ , which is the relevant energy scale characterizing the strongly coupled QGP liquid, is much smaller than the virtuality carried by the energetic partons in the fragmenting shower, and for this reason we will assume that (even while the partons in the shower lose energy to, and exchange momentum with, the plasma as they propagate through it) the structure of the branching shower is unmodified. This simplifying assumption is one of the bases for the hybrid model. It is a good approximation during the early stages of the shower when the virtuality of the partons in the shower is much larger than any virtuality of order  $T$  which is injected by the medium. In the later stages of the shower, it is a simplifying assumption that could be revisited in future work.

As they pass through the plasma, the partons in the jet shower will transfer energy and momentum to the medium at a rate that should be described without assuming weak coupling, since the typical momentum exchange of such interactions is of the order of the temperature  $T$ . In the hybrid model, these processes are modeled by assuming that the rate of energy loss takes on the same form as that for a light quark passing through the strongly coupled plasma of  $\mathcal{N} = 4$  supersymmetric Yang-Mills (SYM) theory with a large number of colors  $N_c$ , the simplest strongly coupled gauge theory with a dual, or holographic, gravitational description. The light quark is described via a string, and energy loss corresponds to parts of the string being absorbed by a black-hole horizon in one higher dimension [93, 105, 107]. This geometric description of parton energy loss yields new intuition and new qualitative insights into the otherwise challenging strongly coupled dynamics of the jet/plasma interaction. For example [107, 109], in this description if two jets have the same energy the one with the wider opening angle loses more energy, similar to a phenomenon that also arises at weak coupling [117–119] and in the hybrid model [113], in those contexts because wider jets contain more partons than narrower ones, and that means that jet quenching results in a population of jets in which narrower jets predominate [109, 118]. The holographic calculations of Refs. [105, 107] also yield a specific analytic form for the rate of parton energy loss, that has then been applied parton-by-parton to the partons in a jet shower in the hybrid model:

$$\left. \frac{dE_{\text{parton}}}{dx} \right|_{\text{strongly coupled}} = -\frac{4}{\pi} E_{\text{in}} \frac{x^2}{x_{\text{therm}}^2} \frac{1}{\sqrt{x_{\text{therm}}^2 - x^2}}, \quad (2.1)$$

where  $E_{\text{in}}$  is the initial energy of the parton before it loses any energy to the plasma and where

$x_{\text{therm}}$  is the jet thermalization distance, or stopping distance, and is given by

$$x_{\text{therm}} = \frac{1}{2\kappa_{\text{sc}}} \frac{E_{\text{in}}^{1/3}}{T^{4/3}}, \quad (2.2)$$

with  $\kappa_{\text{sc}}$  a parameter that depends on the 't Hooft coupling,  $g^2 N_c$ , as well as on details of the gauge theory and of how the energetic parton is prepared. In the hybrid model [111–113],  $\kappa_{\text{sc}}$  is treated as a free parameter that has been fixed by comparing the model predictions for one measured quantity to data, as described below. The parameter  $\kappa_{\text{sc}}$  is the single free parameter in the hybrid model; it controls the magnitude of  $dE/dx$ , the rate of parton energy loss whose form is given by (2.1), and as such its value affects the hybrid model predictions for every observable. The fitted value of  $\kappa_{\text{sc}}$  turns out to correspond to a value of the thermalization length  $x_{\text{therm}}$  for the liquid QGP of QCD produced in heavy ion collisions that is about 3 to 4 times longer than that for the strongly coupled  $\mathcal{N} = 4$  SYM plasma with the same temperature, a result that is not unreasonable given the larger number of degrees of freedom in the latter theory [111–113].

In this Section, we provide a brief description of the hybrid model and how it has been used to calculate how various jet observables are modified in heavy ion collisions relative to proton-proton collisions, as a consequence of the passage of the partons in the jet shower through the plasma produced in a heavy ion collision. A more detailed account of the base model may be found in Refs. [111, 112]. Equation (2.1) gives the rate of energy loss of each parton as it traverses the plasma and, as discussed in Ref. [111], the lifetime of each parton from when it is created at a splitting to when it itself splits is taken to be

$$\tau = 2 \frac{E}{Q^2}, \quad (2.3)$$

with  $E$  the energy of the parton and  $Q$  its virtuality. The factor of 2 connects this equation in the soft limit with the standard expression for the formation time. This prescription, which assigns a space-time structure to the parton shower in terms of the formation times, is supported by certain weak coupling computations, for example the medium induced two gluon inclusive emission calculated in Ref. [124] in which it is seen that the second emission is delayed by precisely the formation time of the parton produced at the first emission. Equations (2.1) and (2.3) together provide the basis for the hybrid model.

In the hybrid model, we begin by taking parton showers generated by simulating collisions in PYTHIA [120] and giving the partons in these showers lifetimes according to Equation (2.3). This gives the shower a structure in space and time. We then place the point of origin of the event generated by PYTHIA at a location in the transverse plane of a heavy ion collision, choosing the location proportional to the number of collisions at that point in the transverse plane. For simplicity, we let the shower evolve without modification for an initial proper time that we take to be  $\tau = 0.6$  fm, and then turn on a medium as described by a hydrodynamic calculation. (See Refs. [111, 112] for the full specification of the hydrodynamic backgrounds that we have used, and references. Here we shall follow Refs. [112, 113].) It would certainly be worth investigating the effects of additional energy loss before the formation of a hydrodynamic medium, but we shall not attempt this here. As the parton shower develops from  $\tau = 0.6$  fm onward, we track the position in space and time of each parton and apply the energy loss  $dE/dx$  from Eq. (2.1), using the local

$T$  taken from the hydrodynamic background at that point in space and time in the expression (2.3) for  $\mathbf{x}_{\text{therm}}$ . We then turn energy loss off for each parton in the shower when the temperature at its location drops below a temperature that we vary between 145 and 170 MeV [111]. If we wish to compute hadronic observables (like fragmentation functions, jet shapes, and missing- $p_T$  observables) as opposed to calorimetric observables like jet  $R_{AA}$ , we hadronize the events with PYTHIA’s Lund String Model. We then run the FastJet anti- $k_t$  algorithm [121, 122] to reconstruct jets, choosing the same value for the reconstruction parameter  $R$  used in whichever experimental analysis we wish to compare to. In essence, choosing a value of  $R$  in the anti- $k_t$  reconstruction algorithm says that clusters of energy should be reconstructed as part of a single jet if they are within  $R$  of each other in the  $\eta - \phi$  plane, with  $\eta$  and  $\phi$  being pseudorapidity and azimuthal angle, respectively.

In order to compare this model to data, we first have to fit its one parameter,  $\kappa_{\text{sc}}$ , which we do by comparing the model predictions for jet  $R_{AA}$  to experimental data. Specifically, we look at  $R_{AA}$  for jets reconstructed with anti- $k_t$  reconstruction parameter  $R = 0.3$  that have transverse momentum in the range  $100 \text{ GeV} < p_T < 110 \text{ GeV}$  and pseudorapidities in the range  $-2 < \eta < 2$  in the 10% most central Pb-Pb collisions with collision energy  $\sqrt{s_{NN}} = 2.76 \text{ TeV}$ . We fix the range for the parameter  $\kappa_{\text{sc}}$  such that the hybrid model results for this specified jet  $R_{AA}$  measurement matches the CMS data point [28, 43], including its error bar.

As discussed in Refs. [111–113], the hybrid model has enjoyed considerable success in modeling the dijet asymmetry, dijet imbalance, photon-Jet observables, and Z-Jet observables, most recently in the remarkably successful comparison made by CMS of hybrid model predictions for various photon-jet observables to a suite of new CMS measurements [41] that appeared after the predictions. All these observables are sensitive to the energy loss, but not to modifications of the shape of the jets. However, even after adding two key effects that are missing from this base framework (transverse broadening and the backreaction of the medium, see below) in Ref. [113], the hybrid model predictions for jet shapes, fragmentation functions, and two missing- $p_T$  observables do not agree quantitatively with data. Several explanations for this were posited in Ref. [113], including the possibility that leaving out the effects of resolution was over-quenching moderate energy partons in the shower as well as the possibility that the wake in the plasma was not fully thermalized as assumed in Ref. [113]. Here, we shall provide an assessment of the first possibility.

Before turning to the effects of resolution, though, we close this Section with a brief review of the two effects added in Ref. [113]. Transverse momentum broadening is the effect that as the partons in the jet shower propagate through the plasma they receive kicks transverse to their direction of motion. As appropriate in a strongly coupled plasma, or for propagation over a sufficiently long distance through a weakly coupled plasma, the transverse momentum picked up by each parton after travelling a distance  $L$  is Gaussian distributed with a width given by  $\sqrt{\hat{q}L}$ , where  $\hat{q} = KT^3$ .  $K$  is a constant at strong coupling and a constant  $\propto g^4$  up to a logarithm at weak coupling. In principle,  $K$  is a new parameter that, like  $\kappa_{\text{sc}}$ , should be fit to data. However, it turns out [113] that jet observables measured to date are relatively insensitive to  $K$  because the softer partons that would receive a noticeable kick are in fact much more affected by energy loss, so much so that the angular-narrowing effects of energy loss (softer partons at larger angles getting fully quenched; wider jets losing more energy than narrower ones) substantially dominate over the angular-broadening coming from transverse kicks. Because its visible effects are small, in the

present paper we shall set  $K = 0$  throughout.

The backreaction of the medium, which is to say the wake left behind in the plasma by the passing jet, is another physical effect that cannot be ignored. The partons in the jet lose energy *and momentum*, which must both be deposited into the medium in the form of a wake. By momentum conservation, this wake must have a net momentum in the jet direction. This means that after hadronization when a reconstruction algorithm is used to reconstruct jets, the reconstructed jets must include some hadrons that come from the hadronization of the wake in the plasma, as well as hadrons coming from the jet itself. This is unavoidable, and must be taken into account in the hybrid model, or in any other model for jet quenching, if one wishes to compare to experimental data on the soft particles in jets and/or the structure of jets at larger angles. In experimental data, there is no way even in principle to separate which of the hadrons that are reconstructed as a jet in fact come from the wake in the plasma. In Ref. [113], the transfer of energy and momentum from hard jet modes to soft plasma modes is assumed to result in a perturbation to the hydrodynamic background that can be treated to linear order, which in turn becomes a linearized perturbation to hadron spectra after hadronization. This perturbation is assumed to have thermalized fully, subject to momentum conservation. After hadronization according to the Cooper-Frye prescription, these assumptions then permit an analytic computation of the contribution to the spectrum of particles in the final state coming from the boosted and heated wake in the plasma that is given by [113]

$$E \frac{d\Delta N}{d^3p} = \frac{m_T}{32\pi T^5} \cosh(y - y_j) \exp \left[ \frac{-m_T}{T} \cosh(y - y_j) \right] \times \left\{ p_\perp \Delta P_\perp \cos(\phi - \phi_j) + \frac{m_T \Delta M_T}{3} \cosh(y - y_j) \right\}, \quad (2.4)$$

where  $p_T$ ,  $m_T$ ,  $\phi$ , and  $y$  are the transverse momentum, transverse mass, azimuthal angle, and rapidity of the emitted thermal particles coming from the wake in the plasma due to the passage of a jet whose azimuthal angle and rapidity are  $\phi_j$  and  $y_j$ .

With a brief look back at the hybrid model in hand, we now turn to our discussion of the resolution length and its incorporation into the hybrid model framework.

### 3 The Resolution Length within QGP

When one parton in a jet shower splits into two, the two offspring will initially be arbitrarily close together. Initially, therefore, they should continue to interact with the plasma as if they were still the single parent parton. Only after they have separated by some distance that we refer to as the resolution length and denote by  $L_{\text{res}}$  will they interact with the plasma independently, as two separate color-charged partons each losing energy and momentum to the plasma. Depending on the opening angle of the splitting, it may take considerably longer than  $L_{\text{res}}/c$  for them to separate from each other by a distance  $L_{\text{res}}$ . Note that, in reality, the physical processes via which the plasma goes from “seeing” one parent to resolving two offspring may be complex and/or quantum mechanical. Our goal here is not a complete description of the resolution process. Rather, in the next Section we shall implement a simplified prescription in which one effective parent parton suddenly becomes two offspring once the offspring are separated by  $L_{\text{res}}$ . We shall describe the



implementation, including its attendant simplifications, there. In this section, we start by asking what the reasonable range of values for  $L_{\text{res}}$  should be.

Because the plasma screens color charges that are separated from each other by more than the Debye, or screening, length  $\lambda_D \equiv 1/m_D$ , with  $m_D$  the Debye mass, we know that  $L_{\text{res}}$  must be of order  $\lambda_D$  or shorter. When two partons are separated by a distance that is greater than  $\lambda_D$ , they must engage with the plasma independently. It is also reasonable to expect that when two partons are much closer than  $\lambda_D$  to each other, well within their own Debye spheres, the medium will not be able to resolve them, but in the case of a weakly coupled plasma this needs further thought, see below.

For the strongly coupled plasma of any theory with a holographic dual,  $\lambda_D$  is of order  $1/T$  and hence is of order the shortest relevant length scale that characterizes the plasma. We therefore conclude that in a strongly coupled plasma,  $L_{\text{res}}$  is indeed of order  $\lambda_D$ , not shorter. For the specific case of strongly coupled  $\mathcal{N} = 4$  SYM theory, the Debye length has been computed holographically in Ref. [123] and is given by  $\lambda_D \approx 0.3/(\pi T)$ . Because the QCD plasma has fewer degrees of freedom, it is reasonable to expect that in temperature regimes where it is strongly coupled, its  $\lambda_D$  is larger by a factor of a few, making it reasonable to estimate that strongly coupled QCD plasma has  $L_{\text{res}} \sim 1/(\pi T)$ .

What about for a weakly coupled plasma? Here  $m_D \sim gT$  meaning that in the strict weak coupling limit the Debye length  $\lambda_D$  is parametrically larger than  $1/T$ , and we should consider whether  $L_{\text{res}}$  could be parametrically smaller than  $\lambda_D$ . One way to gain intuition is to consider the perturbative computations of medium-induced gluon radiation from a dipole, the so-called antenna problem discussed for example in Refs. [114–116, 124]. In these calculations, the gluon radiation is controlled entirely by the summed charge of the dipole if the opening angle of the antenna  $\theta_{\text{ant}}$  is small enough such that  $\theta_{\text{ant}}L \ll L_{\text{res}}$ , with  $L$  the thickness of the medium through which the dipole propagates. That is, if the charges in the dipole never separate by more than  $L_{\text{res}}$ , as a consequence of quantum interference they radiate as if they were a single charge, unresolved by the medium. In the case of a thin medium, this  $L_{\text{res}}$  is indeed given by  $\lambda_D$  [124]. If  $\theta_{\text{ant}}$  is larger and the legs of the antenna separate at a faster rate, the interference rapidly fades away, and the gluon emission spectrum is dominantly that for independent emission from each of the individual antenna charges separately. So, for a thin medium at weak coupling,  $L_{\text{res}} \sim \lambda_D$ .

For a thick medium at weak coupling, however, the argument is more subtle because quantum interference over the course of multiple soft interactions with the medium as a hard parton propagates for a distance  $L$  introduces a new length scale,  $1/\sqrt{\hat{q}L}$ . (See, for example, Refs. [116, 117]. For a review of earlier work going back to Ref. [125] in which this scale appears, see Ref. [59].) Taking  $\hat{q} \sim g^4 T^3$ , we see that  $1/\sqrt{\hat{q}L}$  is shorter than  $\lambda_D \sim 1/(gT)$  only if the hard parton has propagated over an  $L$  that is longer than of order  $1/(g^2 T)$ . (Note that  $L > \mathcal{O}(1/(g^2 T))$  is also the criterion for the medium to be considered thick.) If we return to the antenna problem but now for a thick medium, if  $\theta_{\text{ant}} > \mathcal{O}(g)$  then the two legs of the antenna will reach a separation of order  $\lambda_D$  before they have traveled a distance of order  $1/(g^2 T)$ , meaning that they will be resolved when their separation is of order  $\lambda_D$  and the scale  $1/\sqrt{\hat{q}L}$  never becomes relevant. In the strict weak coupling limit, this argument suffices. We shall take this as sufficient evidence to proceed using the assumption that  $L_{\text{res}} \sim \lambda_D$ , as this is valid in a strongly coupled plasma as well as in a weakly coupled plasma except for the case where  $\theta_{\text{ant}} < \mathcal{O}(g)$  in a plasma that is both thick and weakly

coupled, a case that can be returned to in future work.

In a weakly coupled plasma, the textbook result for  $m_D$  can be found, for example, in Ref. [126] and is given by  $m_D^2 = \frac{3}{2}g^2T^2$  for QCD with  $N_c = N_f = 3$ . Taking  $\alpha_{QCD} \equiv g^2/(4\pi)$  to lie within the broad range from  $\frac{1}{8}$  to  $\frac{1}{2}$  corresponds to taking  $\lambda_D$  to lie within the broad range from  $2.0/(\pi T)$  to  $1.0/(\pi T)$ .

Reflecting these considerations, it seems that

$$\frac{1}{\pi T} \lesssim L_{\text{res}} \lesssim \frac{2}{\pi T} \quad (3.1)$$

is a reasonable range of expectation for  $L_{\text{res}}$  in either a strongly coupled QCD plasma or a weakly coupled QCD plasma. In implementing the effects of resolution in the hybrid model, we shall define

$$L_{\text{res}} = \frac{R_{\text{res}}}{\pi T}, \quad (3.2)$$

treating  $R_{\text{res}}$  as a new parameter in the model. With this parametrization, we ensure that  $L_{\text{res}} \propto 1/T$  in the hybrid model, with  $T$  the local temperature at the position of each parton in the shower at a given time. We will explore the consequences of choosing the proportionality constant  $R_{\text{res}} = 1$  and  $R_{\text{res}} = 2$ , spanning the reasonable range for the resolution length in either strongly coupled or weakly coupled QCD plasma. We shall also explore the consequences of choosing  $R_{\text{res}} = 5$ , corresponding to an unphysically large value of the resolution length. We do so in order to check the robustness of our results, i.e. for the purpose of confirming that none of the results we report are hypersensitive to the value of  $L_{\text{res}}$  that we choose.

## 4 Implementation of the Effects of Resolution within the Hybrid Model

In this Section we will describe our implementation of the effects of resolution within the hybrid strong/weak coupling model, whose main features have already been described in Section 2. Noting that the hybrid model is itself only a model, our goal is not a complete description of the physical processes via which two offspring partons produced in a splitting go from being unresolved to being fully resolved and losing energy separately. Our goal is a simplified prescription that suffices to gauge the magnitude of the effects of including resolution on several physical observables that are of interest and where it is reasonable to expect some effects, with a magnitude to be determined.

Until now, the hybrid model has been built upon a space-time picture for the development of a parton shower that is based solely on the formation time argument (2.3), such that a specific parton splits into its two offspring once the formation time for that parton has passed. This process iterates until all partons are on-shell. Each parton in the shower loses energy independently, according to (2.1), from the moment that it is produced in a splitting. Including the effects of resolution serves to modify the space-time structure of the shower that the medium sees, responds to, and affects. Because it takes time before the offspring from each splitting in the shower are separated by  $L_{\text{res}}$  and resolved, the moments in time when the number of shower partons seen by the medium increases are delayed. The medium now sees the shower as a collection of *effective partons*, each of which is either a single parton that has separated from its siblings by a distance  $L_{\text{res}}$  and is losing energy independently, or a collection of offspring that are still being treated together as a single not-yet-resolved entity, and as such are all losing the same fractional energy. There are

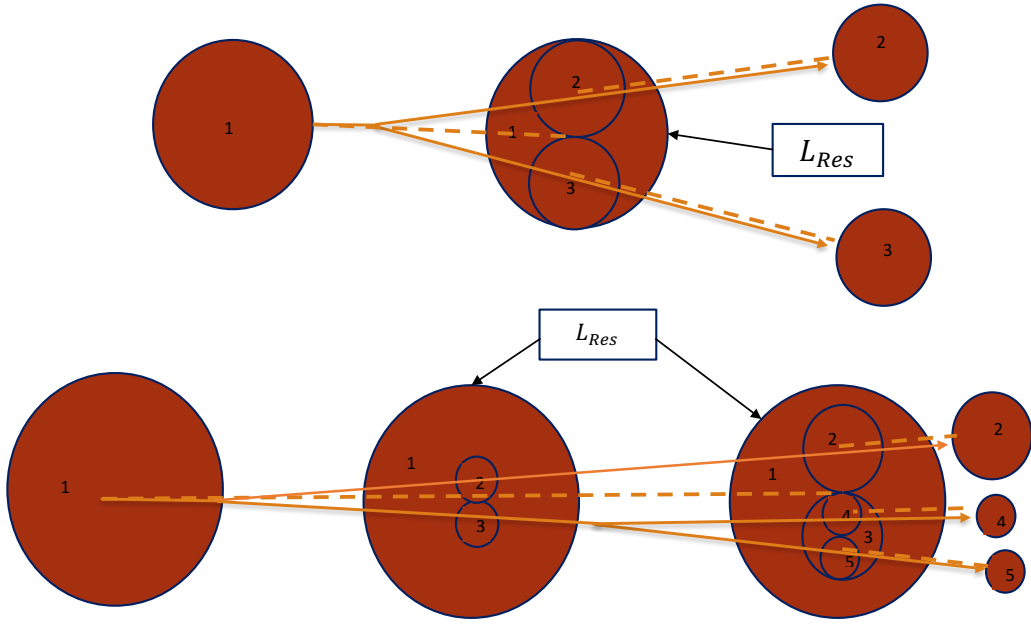


**Figure 1:** A simplified picture illustrating how we implement the effects of resolution. Solid lines indicate the particles in the parton shower, without any consideration of resolution. Dashed lines indicate the new shower seen by the medium after taking into account that it can only resolve offspring partons as distinct when they have separated by a distance  $L_{\text{res}}$ . In the top diagram, particle 1 propagates as a single effective parton after it splits until its offspring, particles 2 and 3, separate by  $L_{\text{res}}$ . In the bottom diagram, particles 2 and 3 have not separated by  $L_{\text{res}}$  before particle 3 splits into particles 4 and 5. It is the later resolution of particles 4 and 5 that “breaks” the effective parton: particle 1 resolves into particles 2, 4, and 5 when this happens.

certainly issues with this oversimplified prescription. The description we have given sounds simple and straightforward only at first hearing; implementing it for a branching shower in a dynamically evolving medium necessitates resolving several important ambiguities. The most obvious one is that when we state that a single effective parton at some location becomes two resolved partons at two separated locations at the moment when the two offspring partons are separated by  $L_{\text{res}}$ , we must specify in which Lorentz frame we are making this statement. This choice has effects and is arbitrary, and the fact that we must make it reflects the oversimplified nature of our treatment of the process of resolution. As we shall see below, our implementation requires us to pick the same Lorentz frame in our treatment of all splittings, and for this reason we shall choose to apply our prescription in the laboratory frame even though in the hybrid model we compute the energy loss of each parton, or effective parton, in its own local fluid rest frame. We describe further ambiguities, and the attendant simplifying assumptions that we make, below.

As the first and simplest example, consider the picture in the upper panel of Fig. 1. Here we find depicted the splitting of parent particle  $m_1$  into sibling particles  $s_2$  and  $s_3$ . The solid orange lines show the “true” trajectory of the partons in the system, determined by the formation time argument only. If instead we require  $s_2$  and  $s_3$  to be spatially separated by more than  $L_{\text{res}}$  in order to be treated as individual resolved objects from the point of view of the medium, we get the

“effective” trajectories shown by the dashed orange lines: the medium perceives that  $m_1$  has lived for a time  $\tau_r$ , which is longer than the formation time  $\tau_f$ , and sees particles  $s_2$  and  $s_3$  simultaneously pop up at  $\tau_r$  at separated spatial locations. Therefore, when we apply our energy loss prescription (2.1) to this system, we will need to quench  $m_1$ , with its summed color charge, momentum vector and (decreasing) total energy, as if it had propagated until  $\tau_r$  before splitting. And, after its energy loss is propagated to its two now separated offspring at  $\tau_r$ , each of its offspring in turn loses energy according to (2.1) starting from  $\tau_r$ . Only after  $\tau_r$  do we have two effective partons, losing energy independently.

In order to determine  $\tau_r$ , we need to check at each time step after the splitting at  $\tau_f$  whether the spatial separation between the offspring  $s_2$  and  $s_3$  (a non-local quantity) is greater than  $L_{\text{res}}$ , a quantity that depends on the local temperature of the plasma. As we already noted, we need to decide in which Lorentz frame to make this check: we evaluate the spatial distance  $\Delta x$  between  $s_2$  and  $s_3$  at the same time, but at the same time in which frame? Once we consider a shower with multiple splittings, the simplest way of avoiding reintroducing ambiguities from the nonlocality of our prescription is to make the same choice of frame for all splittings. We choose to use the laboratory frame. Furthermore, we need to decide which temperature to use in defining  $L_{\text{res}}$ : we choose the temperature at the location of the effective parton,  $m_1$ , (the dashed orange line) at the same laboratory frame time at which we are measuring  $\Delta x$ , the spatial separation between  $s_2$  and  $s_3$ .  $\tau_r$  is then the laboratory frame time at which  $\Delta x$  has become equal to  $L_{\text{res}}$ . This completes the specification of our simplified implementation of resolution — for the simple case depicted in the top panel of Fig. 1.

We turn now to a more involved, and in fact more realistic situation, where further splittings occur before the first two offspring are resolved from each other. This situation is illustrated in the lower panel of Fig. 1. Consider  $m_1$  splitting into  $s_2$  and  $s_3$ , where  $s_3$  splits into  $d_4$  and  $d_5$  before  $\Delta x_{23}$ , the spatial separation between  $s_2$  and  $s_3$ , becomes greater than  $L_{\text{res}}$ . In this example, the first separation to exceed its relevant  $L_{\text{res}}$  is the one between  $d_4$  and  $d_5$ , namely  $\Delta x_{45}$ , and not  $\Delta x_{23}$ . Of course, the reader will observe that before  $\Delta x_{45} > L_{\text{res}}$ ,  $s_2$  and  $d_5$  may separate by  $\Delta x_{25} > L_{\text{res}}$ , and one could imagine this causing the resolution. The reason why we don’t attempt to specify a prescription based upon this is that when  $d_5$  resolves from  $s_2$ ,  $d_4$  is still unresolved both from  $s_2$  and  $d_5$ , meaning that there would be an ambiguity regarding the arrangement of these three partons into effective partons: should  $d_4$  belong to an effective parton together with  $s_2$ , or to one together with  $d_5$ ? In order to avoid these and several other ambiguities arising from our phenomenological approach to the problem, we prescribe that the resolution check is to be done only between closest relatives, building effective partons from sibling particles that can in turn be combined with *their* siblings to form even larger effective partons. In the example shown in the lower panel of Fig. 1, we never consider the distances  $\Delta x_{24}$  or  $\Delta x_{25}$ . As long as  $\Delta x_{45} < L_{\text{res}}$ , we treat  $d_4$  and  $d_5$  as an unresolved effective parton. And, as long as the distance between this effective parton and  $s_2$  is less than  $L_{\text{res}}$ , the three particle system behaves as a single effective parton, following the trajectory of  $m_1$ . This persists until the moment when  $\Delta x_{45} > L_{\text{res}}$ , where particles  $s_2$ ,  $d_4$  and  $d_5$  suddenly appear. Thus, in this example particle  $s_3$  is never seen by the plasma as an independent parton losing energy in its own right. Indeed, resolving  $d_4$  and  $d_5$  has caused  $s_2$  and  $s_3$  to be resolved since, at that point,  $s_3$  no longer exists as an effective parton that could be paired with  $s_2$ . The algorithm that we have described via this example is not the only

possible way in which to implement the effects of resolution. Its principle virtue is that it is fully specified, with no remaining ambiguities, and as such will meet our needs. Recall that our goal is a simplified prescription that we can use to gauge the magnitude of the effect of including a nonzero  $L_{\text{res}}$  on various observables.

Let us now walk through the logic of the algorithm that we shall follow to modify the space-time structure of any shower, generalizing beyond the examples depicted in Fig. 1. First, we fully reconstruct the parton shower by calculating each particle’s initial and final position, initial momentum, parent particle, creation time, and splitting (or finishing) time, exactly as in the standard hybrid model approach, treating every parton as independent from the moment when it is created at a splitting — without regard for resolution. We then step through time incrementally, starting from when a parent splits into its offspring. At each time step we recalculate  $L_{\text{res}}$  from the temperature at the parent’s position, and we advance the offspring particles’ positions according to their initial velocity, which the energy loss procedure (2.1) from the hybrid model keeps constant.<sup>1</sup> Note also that we make no changes to the shower before  $\tau = 0.6 \text{ fm}/c$  since before this time we have no hydrodynamic medium and no parton energy loss in the model. In effect, we take  $L_{\text{res}} = \infty$  before  $\tau = 0.6 \text{ fm}/c$  and choose  $L_{\text{res}} = R_{\text{res}}/(\pi T)$  at  $\tau = 0.6 \text{ fm}/c$ , and from then onward. Starting at  $\tau = 0.6 \text{ fm}/c$  and at each time-step thereafter, we ask whether each set of sibling partons is resolved or unresolved, and if they are unresolved we group them into an effective parton. We record the first time-step at which the separation between a pair of offspring exceeds  $L_{\text{res}}$ , with  $L_{\text{res}}$  defined in terms of the temperature at the location of their parent effective parton. This is the time after which each offspring will begin to lose energy independently. We also record the position of each of the offspring at this time. After applying this procedure throughout, we record the modified lifetimes (from the time when a parton first begins to lose energy independently at its own resolution time until the time when it is replaced by its two independent offspring at their resolution time) for each of the particles in the shower.

At each time step, we require that each parent in the branching tree must be resolved if any of its offspring have been resolved. If a pair of offspring are resolved before their parent, we set the resolution time of the parent to that of the offspring, in effect setting the modified lifetime of the parent to zero. (For an example, consider  $s_3$  in the lower panel of Fig. 1.) At each time step, we also enforce that sibling particles must resolve at the same time, so that if one sibling’s resolution is forced by one of its children or grandchildren, then the other sibling’s is as well; if a violation is found, we set the later resolution time equal to the earlier. We keep reapplying these two checks in alternation until doing so does not change anything, and only then proceed. With the continued application of these two checks, when offspring particles resolve they force the resolution of their parent particle, and their parent particle’s parent, and so on. Thus, sibling particles very late in the event which separate very rapidly from each other can drastically change the resolution time of every particle in the siblings’ lineage.

---

<sup>1</sup>This is true only when transverse broadening, described in Section 2 and parametrized by  $K$ , is absent. If  $K \neq 0$ , the resulting kicks to the transverse momentum of the partons in the shower would change their velocity vectors, and would introduce changes to the separation between offspring partons as they propagate through the plasma. The calculations of Ref. [113] indicate that including a nonzero  $K$  has negligible effects on all the observables that we shall consider in this paper. For this reason, as well as because including  $K \neq 0$  would considerably complicate our implementation of resolution effects, we set  $K = 0$  throughout this paper.

After stepping through the entire history of the branching tree, applying the algorithm that we have just described, we end up with a new tree, with new creation times and positions for offspring particles (at the moment when they were resolved), and new lifetimes for each particle in the tree. We then quench this new shower, applying the energy loss rate (2.1) to the partons (effective partons) in this new shower using their new positions, creation times, and lifetimes but otherwise following the hybrid model algorithm as described in Section 2 and Refs. [111–113].

Now that we have explained the algorithm via which we shall model the effects of resolution in the hybrid model, an algorithm that has the virtue of being fully specified with no remaining unresolved ambiguities but that is surely not unique, we are ready to look at how turning on  $L_{\text{res}} \neq 0$  modifies the predictions of the model for some important jet observables.

## 5 The Effects of Resolution on Jet Observables

As already outlined in Section 2, the analysis of resolution effects in this work is built on top of the hybrid model without transverse broadening effects, but with particles originating from the backreaction of the medium — the wake that the jet creates in the plasma — included. Results for observables are obtained from hadrons that come from the hadronization of the parton showers originating in hard collisions as well as those that come from the hadronization of the medium, including in particular the perturbations originating from the wake. In order to compare to data, before reconstructing jets we need to perform a background subtraction, using the same techniques for doing so that the experimentalists have used in their analysis of whichever observable we wish to compare to. The details of these procedures are described in Ref. [113].

### 5.1 Distribution of energy lost by partons in a jet

Before turning to actual jet observables, we want to begin by getting some insight into how increasing  $L_{\text{res}}$  affects the distribution of the amount of energy lost by the set of partons in the final state of the parton shower (i.e. the on-shell partons that are ready to hadronize) within a high energy jet. For each such final parton coming from the parton shower we define the quantity  $\lambda \equiv E_Q/E_V$ , where  $E_V$  is the energy that this particular parton would have had had in vacuum, in the absence of any medium, and  $E_Q$  is the quenched energy that this particular parton has after it has propagated through the medium. (This is a quantity that we can look at within our model calculation. It cannot be determined in experimental data, of course, because experimentalists do not see partons, because even if they did they would have no way of knowing whether a final parton came from the parton shower, and because even if they did they would have no way of knowing  $E_V$ .) Now, if all the partons within a jet had lost the same fraction of their energy, which is to say if all of them had behaved throughout as a single effective parton as would be the case for  $L_{\text{res}} \rightarrow \infty$ , then every final parton in the shower would have the same  $\lambda$ . Therefore, one way to see that because  $L_{\text{res}}$  is finite some partons within the shower have indeed been resolved, and treated independently by the medium, is to compute, jet-by-jet, the distribution of the quantity  $\lambda/\langle\lambda\rangle$ . Here,  $\langle\lambda\rangle$  is the average of  $\lambda$  for all the partons in a single jet. We can then compute the  $\lambda/\langle\lambda\rangle$  distribution averaged over many jets. We show the result in Fig. 2 for jets with  $p_T > 100$  GeV reconstructed by applying the anti- $k_t$  algorithm with  $R = 0.3$  to the partonic final state from our hybrid model with four different values of  $R_{\text{res}} \equiv L_{\text{res}}\pi T$ , namely 0, 1, 2 and 5. As expected, the larger the value of  $R_{\text{res}}$  the more

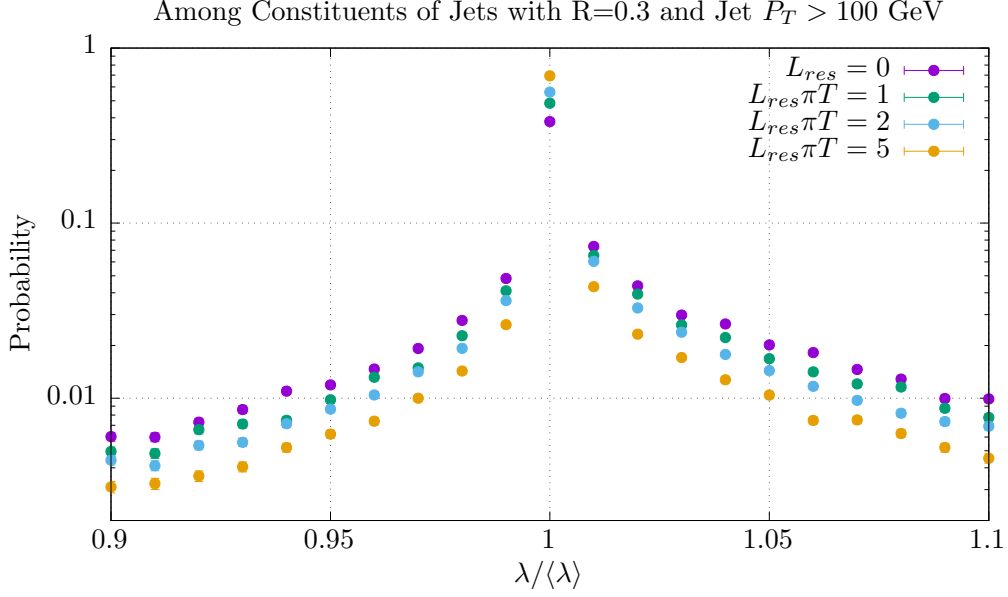


**Figure 2:** To illustrate the effects of resolution, we plot the distribution of  $\lambda/\langle\lambda\rangle$  averaged over a sample of jets with  $p_T > 100$  GeV from 0-5% centrality collisions with  $\sqrt{s_{NN}} = 2.76$  TeV. We have quenched the partons in the jet showers using the hybrid model with varying values of  $L_{\text{res}}$ , in all cases with the fitted value of  $\kappa_{\text{sc}}$ .  $\lambda$  is the ratio of the energy of a particular parton after quenching to the value it would have had in the absence of the medium;  $\langle\lambda\rangle$  is the average of  $\lambda$  over all the partons in a single jet. As the resolution length  $L_{\text{res}}$  increases, more and more of the partons within any given jet remain unresolved, behaving as a single effective parton and losing the same fractional energy. Hence, as  $L_{\text{res}}$  is increased this distribution tends toward a  $\delta$  function at 1. (Even as  $L_{\text{res}} \rightarrow \infty$  it does not become a true  $\delta$  function, though, because the partons reconstructed as a jet are not all descendants of a single parent parton.)

this distribution peaks around  $\lambda/\langle\lambda\rangle = 1$ , getting closest to a  $\delta$  function distribution for the case  $R_{\text{res}} = 5$ . Note that not all of the partons that are reconstructed as part of a particular jet come from a single parent parton from the hard scattering; some come from initial state radiation, or even from a different parton from the hard scattering. For this reason, even when  $R_{\text{res}}$  is as large as 5 the distribution has significant tails.

The reader will observe that in the opposite limit, when  $L_{\text{res}} = 0$  and the medium perfectly resolves the partons in the shower as in the unmodified hybrid model, treating each parton as losing energy independently from the instant that it is created in a splitting, the distribution in Fig. 2 is already fairly peaked around 1. There are two reasons for this. First, the partons that lose all their energy to the medium and do not make it into the final state of the quenched shower are excluded from this plot; only those that survive, and hence can be reconstructed as belonging to a jet, can contribute. Many partons that were resolved by the medium and have a  $\lambda$  well below  $\langle\lambda\rangle$  therefore do not end up counted in the histogram plotted in Fig. 2. The second reason arises from the bias imposed by looking only at reconstructed jets with  $p_T$  above some cut, here 100 GeV. This cut, together with the fact that the jet spectrum falls steeply with  $p_T$ , biases the sample of jets toward those whose initial energy was not far above 100 GeV and which did not lose much

energy. Since wider jets [107, 109] containing more, and softer, partons lose more energy than narrower jets containing fewer harder partons [113, 118], this selection criterion biases the sample toward narrow jets containing fewer harder partons which are less likely to separate from each other sufficiently to be resolved and which travel longer distances before they themselves split.

## 5.2 Jet $R_{AA}$ , including its Dependence on the Jet Reconstruction Parameter $R$

Turning now to experimental observables, henceforth in all analyses that we report we include particles coming from the medium perturbed by the wake left in it by the jet as well as particles coming from the parton shower. Note that for all observables that we look at in this paper, we will focus on Pb-Pb collisions with  $\sqrt{s_{NN}} = 2.76$  TeV.

The first observable that we must calculate is the jet  $R_{AA}$ , because we use the experimental measurement of this observable to fix  $\kappa_{sc}$ , the parameter that controls the magnitude of the energy loss in the hybrid model, see Eq. (2.1). As we noted in Section 2, in the hybrid model we fix  $\kappa_{sc}$  by matching the predictions of the hybrid model to the CMS measurement of jet  $R_{AA}$  for jets reconstructed with the anti- $k_t$  reconstruction parameter  $R = 0.3$  that have  $100 \text{ GeV} < p_T < 110 \text{ GeV}$  in the 10% most central Pb-Pb collisions [28, 43]. We obtain four different values of  $\kappa_{sc}$  by matching the predictions of the hybrid model for this one data point to the upper and lower ends of the CMS error bar and doing so with the temperature at which we turn quenching off set to 145 MeV and 170 MeV. As in Refs. [111–113], for any observable that we look at later, we calculate the predictions of the hybrid model using the highest and the lowest of these four values of  $\kappa_{sc}$ , in so doing obtaining a band for the hybrid model prediction that encompasses the experimental error in the measured data point that we use to fix  $\kappa_{sc}$  plus a crude estimate of what can loosely be considered a theoretical systematic error coming from the model [111, 112].

Here, we must fix the fitted range for  $\kappa_{sc}$  anew for each nonzero value of  $L_{res}$  that we employ, namely  $L_{res} = R_{res}/\pi T$  with  $R_{res} = 1, 2, \text{ and } 5$ . Without doing the calculation, it is not obvious whether the fitted values of  $\kappa_{sc}$  should increase or decrease with increasing  $R_{res}$ . Increasing  $R_{res}$  means that various parent partons live longer, and can lose fractionally more energy, since in the expression (2.1) for  $dE/dx$  the rate of fractional energy loss increases with increasing  $x/x_{therm}$ . But, it also means that twice as many offspring partons live less long, and hence lose less energy. If the first effect were to dominate,  $\kappa_{sc}$  would need to be reduced as  $R_{res}$  is increased, in order to maintain the fit to the experimentally measured jet  $R_{AA}$  data point, with its error bar. In fact, what we find instead is that the fitted range for  $\kappa_{sc}$  increases modestly with  $R_{res}$ , increasing relative to its  $R_{res} = 0$  range of  $0.323 < \kappa_{sc} < 0.421$  by about 6-7%, 9-10% and 13-16% for  $R_{res} = 1, 2$  and 5. The fact that the fitted range of  $\kappa_{sc}$  increases slightly with increasing  $L_{res}$  indicates that the consequence of including a nonzero resolution length  $L_{res}$  that impacts jet energy loss most is the fact that various offspring partons have shorter lifetimes and so lose less energy. In order to fit the jet  $R_{AA}$  experimental data point, the reduction in the number of effective partons caused by delaying the appearance of offspring partons as effective partons until they have been resolved and thus shortening the lifetime of the offspring partons as effective partons losing energy independently) needs to be compensated by increasing  $\kappa_{sc}$  so as to shorten the thermalization distance (2.2) in the hybrid model, increasing the rate of energy loss for all partons.

With  $\kappa_{sc}$  fixed, the simplest observable for us to compute is the jet  $R_{AA}$ , but now using varying values of the anti- $k_t$  reconstruction parameter,  $R$ . Reconstructing a jet sample using a smaller value



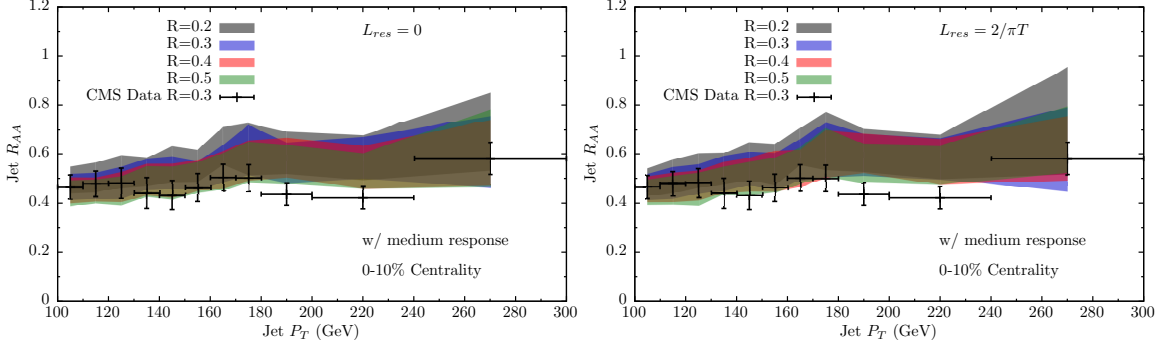


**Figure 3:** Jet  $R_{AA}$  as a function of jet  $p_T$  for various values of the reconstruction parameter,  $R$ , for  $L_{res} = 0$  (left panel) and  $L_{res} = 2/\pi T$  (right panel). We see that wider jets tend to lose more energy than narrower jets. Including the effects of resolution does not affect this conclusion.

of  $R$  yields a sample in which narrower jets dominate, for two reasons: nearby clusters are more likely to be counted as separate jets, and the full energy of a wider jet may not be reconstructed, making it less likely for wider jets to pass the  $p_T$  cut. We show our results in Fig. 3, with  $L_{res} = 0$  and with  $L_{res} = 2/\pi T$ . In both panels, the blue band agrees with the left-most CMS data point because we have used this point to fit  $\kappa_{sc}$ . We see that wider jets tend to lose more energy than narrower jets, resulting in more suppression of their  $R_{AA}$ . (One may speculate that increasing  $R$  and reconstructing wider jets could mean catching more of the “lost” energy within the reconstructed jets, which would mean less suppression of jet  $R_{AA}$ . Clearly this effect does not dominate, at least up to  $R = 0.5$ . Much of the “lost” energy ends up at larger angles relative to the jet axis.) The result that wider jets tend to lose more energy than narrower jets in the hybrid model was already noted in Ref. [113]; here we see that this conclusion remains unchanged, and in fact the hybrid model results for  $R_{AA}$  are hardly modified, when we include resolution effects — as long as we refit  $\kappa_{sc}$ . This is an indication of the robustness of the hybrid model, including in particular the procedure of fitting the single parameter that controls the rate of energy loss to an experimentally measured jet  $R_{AA}$  data point. (The conclusion that wider jets lose more energy also arises for holographic jets [107, 109]; and, the conclusion that jets containing more effective partons lose more energy also arises at weak coupling [118, 119].) It is also worth noting that the  $R$ -dependence of jet  $R_{AA}$  that we find — namely slightly less suppression of  $R_{AA}$  for the narrower jets reconstructed using smaller values of  $R$  — is similar to what has been seen in recent measurements from CMS [43], although at present the error bars are too large relative to the smallness of the  $R$ -dependence to allow for a definitive statement. Increased precision for this type of measurement is important as it could yield further confirmation that narrower jets lose less energy, and that the lost energy seems to efficiently end up at large angles relative to the jet direction, for example as in a strongly coupled picture in which the lost energy ends up in a hydrodynamic wake in the plasma.

### 5.3 Fragmentation functions and jet shapes

We have seen in the previous two Subsections that the important consequence of introducing the effects of resolution comes from the fact that the time when the medium notices that a parent parton has split into two offspring is delayed until the offspring partons can be resolved, meaning

that partons with moderate energies have less time to lose energy independently. Because they spend more time losing energy as a part of their larger parental effective parton before becoming independent, they are more likely to lose only the same fraction of their energy as the jet as a whole, not more (Section 5.1). As a second consequence, the total energy lost by the jet as a whole is reduced, but this is compensated for in the hybrid model by increasing  $\kappa_{\text{sc}}$ , the parameter that controls the magnitude of parton energy loss (Section 5.2) in order to maintain the fitted agreement between the hybrid model prediction for jet  $R_{AA}$  and data. Both because of this compensation via increasing  $\kappa_{\text{sc}}$  and because they survive longer as effective partons, the hardest, most energetic, partons in the core of the jet suffer a modest increase in their energy loss.

The modification of the spacetime structure of the jet parton shower, as perceived by, modified by, and responded to by, the strongly coupled liquid QGP in which it finds itself resulting from introducing the effects of resolution should manifest itself in modifications to various intra-jet observables, to which we now turn. Based on what we have seen in Sections 5.1 and 5.2, we expect that, relative to previous hybrid model studies in which  $L_{\text{res}} = 0$ , once we turn on a nonzero  $L_{\text{res}}$  the moderate energy partons in the jet should lose somewhat less energy and should be more likely to survive into the final state, where they can hadronize and be seen as moderate energy hadrons within the reconstructed jets. Correspondingly, the few hardest partons and hence hadrons should lose a little bit more energy. After hadronization, we should expect to see both effects in the fragmentation function. Also, to the extent that the few hardest partons define the center of the jet and the moderate energy partons are more spread out in angle around that center, we should also expect to see both effects in the jet shape. We therefore look at how the hybrid model predictions for these two intra-jet observables are modified once we turn on a nonzero  $L_{\text{res}}$ .

We begin with the jet fragmentation function, which characterizes the fraction of the longitudinal energy of the jet carried by individual charged hadrons within a jet. The tracks used in the analysis lie within a distance  $r < R = 0.3$  from the jet axis in the  $\eta - \phi$  plane, and the distribution is expressed in terms of the variable  $\ln(1/z)$ , with  $z$  defined as  $z \equiv p_{\text{track}} \cos \theta / p_{\text{jet}}$ , where  $\theta$  is the angle between the momentum vector of the track and the jet axis as defined via the anti- $k_t$  reconstruction. In Fig. 4, we show the ratio of the quenched fragmentation function for jets in heavy ion collisions to the fragmentation function for jets produced in p-p collisions that propagate in vacuum. In the right panel, we include the effects of the wake in the strongly coupled plasma that the jet creates since, as described in Section 2, some of the hadrons that come from the hadronization of the plasma including this wake must end up included in the reconstructed jet. In the left panel, we do not include this response of the medium to the jet. In both panels, the previous predictions of the hybrid model with  $L_{\text{res}} = 0$  are shown in grey, whereas our results for the physically well-motivated values of the resolution length,  $L_{\text{res}} = 1/\pi T$ , and  $L_{\text{res}} = 2/\pi T$  are shown in blue and red. The orange band corresponds to the unphysically large value  $L_{\text{res}} = 5/\pi T$ . We see in Fig. 4 that, as expected, the contribution from the hardest tracks lying around  $z \lesssim 1$  is diminished by increasing  $L_{\text{res}}$ , while the contribution of the softer particles with moderate energies around  $\ln(1/z) \sim 3$  is enhanced. Including the effects of resolution shifts the predictions of the hybrid model in the direction of the CMS data [33], but the rise seen in the CMS data at the smallest  $z$  (largest  $\ln(1/z)$ ) is not fully explained. We also see that in this regime the contribution coming from including the backreaction of the medium, the wake in the plasma, is larger in magnitude than the contribution coming from including the effects of resolution. For the hardest hadrons with

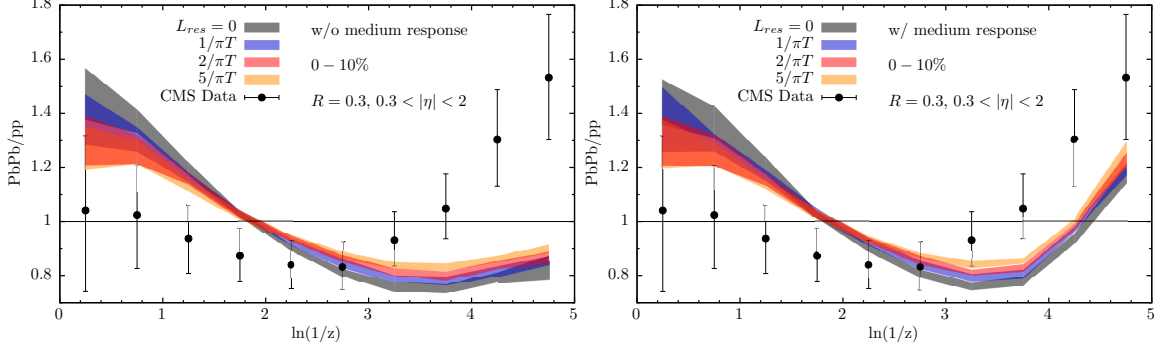


**Figure 4:** Fragmentation functions characterize the probability distribution for the longitudinal energy fraction  $z$  carried by an individual hadron relative to the total energy of the jet. We plot the ratio of the fragmentation function for jets reconstructed with the anti- $k_t$  parameter  $R = 0.3$  that have  $p_T^{\text{jet}} > 100$  GeV and  $0.3 < |\eta| < 2$  in the 10% most central Pb-Pb collisions to that in p-p collisions with the same 2.76 TeV collision energy. In the left panel, we only include hadrons coming from the hadronization of the jet showers. In the right panel, we also include hadrons coming from the medium after background subtraction, meaning that we see the effects of the wake that the jet leaves behind in the plasma. In both panels, we show the predictions of the hybrid model with  $R_{\text{res}} = L_{\text{res}}\pi T$  given by 0, 1, 2 and 5. Turning on a nonzero  $L_{\text{res}}$  has allowed more hadrons carrying a smaller fraction of the jet energy to survive into the final state, seen on the right of each panel, and has correspondingly reduced the contribution of hadrons carrying a large fraction of the jet energy, seen on the left. Including the effects of resolution shifts the predictions of the hybrid model in the direction of the CMS data [33], but the effects are relatively small in magnitude, in particular for  $R_{\text{res}} = 1$  and 2 which corresponds to our range of expectations for the resolution length  $L_{\text{res}}$ .

$z \lesssim 1$ , on the left, the two effects both push the predictions of the model downward and together bring them quite close to the CMS data.

We turn next to the jet shape observable, which quantifies the fraction of the total energy of jets reconstructed with anti- $k_t$  parameter  $R$  that lies within an annulus of radius  $r$ , and width  $\delta r$  (in  $\eta - \phi$  space), centered on the jet axis. Following Ref. [30], we define the differential jet shape as

$$\rho(r) \equiv \frac{1}{N_{\text{jets}}} \frac{1}{\delta r} \sum_{\text{jets}} \frac{\sum_{i \in r \pm \delta r/2} p_t^{i, \text{track}}}{p_t^{\text{jet}}} \quad (5.1)$$

for  $r < R$ , where the particles in the sum are all the hadrons found in the specified annulus (after background subtraction) whether or not they were identified as constituents of the jet by the anti- $k_t$  algorithm.  $\rho(r)$  is defined such that it is normalized to one. In Fig. 5, we show the ratio of the jet shape for quenched jets in heavy ion collisions to that for jets produced in p-p collisions that propagate in vacuum. For reference, the experimental results for this ratio are also shown, as measured by the CMS collaboration [30]. In the right panel we include the effects of the wake in the strongly coupled plasma, and in the left panel we do not include this response of the medium to the jet. As in Fig. 4, in both panels of Fig. 5 the colored bands show how the predictions of the hybrid

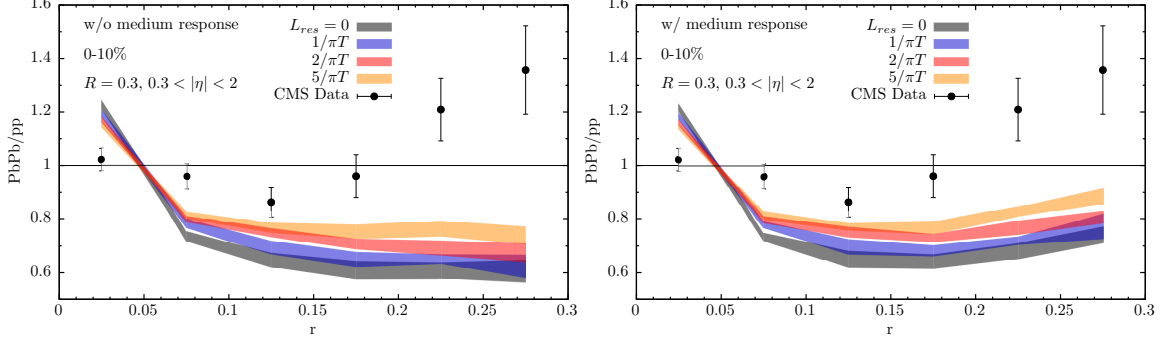


**Figure 5:** The jet shape observable characterizes the angular distribution of energy within the jet as a function of  $r$ , the angle in the  $\eta - \phi$  plane relative to the jet axis. We plot the ratio of the jet shape for jets reconstructed with the anti- $k_t$  parameter  $R = 0.3$  whose centers lie within  $0.3 < |\eta| < 2$  and that have  $p_T^{\text{jet}} > 100$  GeV in the 10% most central Pb-Pb collisions to that in p-p collisions with the same 2.76 TeV collision energy. In the left panel, we only include hadrons coming from the hadronization of the jet showers. In the right panel, we also include hadrons coming from the medium after background subtraction, seeing the effects of the wake in the plasma. In both panels, we show the predictions of the hybrid model with  $R_{\text{res}} = L_{\text{res}}\pi T$  given by 0, 1, 2 and 5. Turning on a nonzero  $L_{\text{res}}$  has allowed more hadrons at larger angles relative to the jet axis to survive into the final state, see the right of each panel, and has correspondingly reduced the contribution of hadrons at the very center of the jet, see the left of each panel. Including the effects of resolution shifts the predictions of the hybrid model in the direction of the CMS data [30], but the effects are relatively small in magnitude, in particular for  $R_{\text{res}} = 1$  and 2 which corresponds to our range of expectations for the resolution length  $L_{\text{res}}$ .

model change for  $R_{\text{res}} = 0, 1, 2$  and 5. As expected, increasing  $L_{\text{res}}$  increases the probability to find hadrons at larger angles relative to the jet axis (and, as seen above, with moderate energies) making it into the detector and therefore into the jets. The energy fraction at the very core of the quenched jets is depleted as a function of increasing  $L_{\text{res}}$  and the contributions in wider annuli are enhanced. It remains the case, though, that because we are comparing quenched and unquenched jets with the same final energy, because narrower jets lose less energy, and because the jet spectrum falls rapidly with energy, there is a bias toward finding quenched jets that are narrower than the unquenched jets. That is, the unquenched jets that were wider lose more energy and end up below the  $p_T^{\text{jet}}$  cut used in the analysis, making the jet shape after quenching narrower than that in p-p collisions. As for the fragmentation function, including the effects of resolution shifts the predictions of the hybrid model for the jet shape seen in Fig. 5 in the direction of the CMS data [30], but the rise seen in the CMS data at larger angles is not fully explained. We also see that in this regime the contribution coming from including the backreaction of the medium, the wake in the plasma, is comparable in magnitude to the contribution coming from including the effects of resolution.

In the case of both the fragmentation function and the jet shape, including the effects of resolution pushes the predictions of the hybrid model in the direction of the data but the effects are modest in magnitude meaning that the interesting qualitative differences between the predictions of the model and the data that were noted in Ref. [113] remain.

## 5.4 Two missing- $p_T$ observables

Ref. [113] also provides hybrid model calculations of a suite of intra-jet observables known collectively as missing- $p_T$  observables. These characterize the distribution in momentum and angle of all the particles in an event containing a pair of reconstructed jets, a dijet, with respect to the axis defined by the dijet [39]. These are excellent observables with which to study the response of the plasma to the jet: if one does not include the hadrons coming from the wake in the plasma in the analysis, the predictions of the hybrid model for these observables are in gross disagreement with experimental measurements [113]; however, upon including the hadrons coming from the wake treated as in Ref. [113] as summarized in Section 2, one obtains broad qualitative agreement with the data while at the same time seeing very interesting remaining discrepancies. The treatment of the wake assumes that the energy and momentum deposited in the plasma equilibrates (more precisely, hydrodynamizes) subject to energy and momentum conservation, and that the resulting perturbation to the hydrodynamic flow and the consequent perturbation to hadron spectra after hadronization are both small enough to be treated to linear order. The authors of Ref. [113] speculate that the interesting discrepancies between hybrid model predictions and the experimental data could be ameliorated either by including the effects of resolution or by improving the analysis of the wake, in particular by taking into account the possibility that the wake does not fully equilibrate. After all, a part of the wake must be created not long before the jet exits the fluid and/or not long before the fluid+wake hadronizes, meaning that some of the wake will have very little time to hydrodynamize. Here, we evaluate the effects of resolution and show that they are small in magnitude relative to the discrepancies in question. This provides indirect support for the suggestion that further analysis of these discrepancies will give us experimental access to the processes via which the wake — a perturbation to the hydrodynamic, strongly coupled, QGP — relaxes by taking a snapshot of these processes before they are complete.

The missing- $p_T$  observables are distributions of averages of the quantity  $\not{p}_T^\parallel$ , calculated for every track in the event and defined as

$$\not{p}_T^\parallel \equiv -p_T \cos(\phi_{\text{dijet}} - \phi) , \quad (5.2)$$

where  $p_T$  and  $\phi$  are the transverse momentum and the azimuthal angle of the track, respectively, and  $\phi_{\text{dijet}}$  is the direction defined by the dijet, namely the bisection of the azimuthal angle between the leading jet angle,  $\phi_{\text{leading}}$ , and the flipped subleading jet azimuthal angle,  $-\phi_{\text{subleading}}$ . With this definition, tracks in the subleading jet hemisphere give positive contributions to  $\not{p}_T^\parallel$ , while those in the leading jet hemisphere contribute negatively. If, as is natural, the hard partons in the subleading jet have lost more energy than those in the leading jet, that drives the average  $\not{p}_T^\parallel$  of hard particles negative. If, correspondingly, the wake created by the subleading jet, with momentum in the same direction by momentum conservation, is larger than the wake created by the leading jet, that drives the average  $\not{p}_T^\parallel$  of soft hadrons coming from the wakes positive. We consider dijet pairs reconstructed from hadrons lying within  $|\eta| < 2.4$  with leading and subleading transverse momenta  $p_T^{\text{leading}} > 120$  GeV and  $p_T^{\text{subleading}} > 50$  GeV respectively and with both jet axes within  $|\eta| < 2$ . We also enforce a back-to-back criterion of  $|\phi^{\text{leading}} - \phi^{\text{subleading}}| > 5\pi/6$  between the two jets. Although we initially consider all jets whose axes lie within  $|\eta| < 2$ , we subsequently make a further cut that restricts our sample of dijets to those for which both jet axes lie within  $|\eta| < 0.6$ . (We use

the larger pseudorapidity range initially to maximize the chance that we do indeed find the two highest energy jets in the event; we use the smaller range for the analysis in order to be able to look at hadrons out to relatively large angles away from the dijet axis.) These are the same cuts used in the analysis of experimental data in Ref. [39].

In the upper and middle two rows of panels in Fig. 6, we show our hybrid model results for the difference in the distribution of  $\langle \not{p}_T^\parallel \rangle$ , which is called the missing- $p_T$  and is the average of  $\not{p}_T^\parallel$  over tracks, in Pb-Pb versus p-p collisions as a function of  $\Delta$  (the angular separation of the tracks in the  $\eta - \phi$  plane with respect to either the leading or the subleading jet axis, depending on which yields a smaller  $\Delta$ ) for dijet events reconstructed with different anti- $k_t$  radii  $R$ . In the upper panels,  $L_{\text{res}} = 0$ ; these are the results of Ref. [113]. In the middle panels,  $L_{\text{res}} = 2/\pi T$ ; these are our results, including the effects of resolution. The lower row of panels shows the experimental measurements published by the CMS collaboration [39]. The contributions to  $\langle \not{p}_T^\parallel \rangle$  are further sliced into different  $p_T$  bins, represented by the different colors, whose sum is shown by the black dots. Although there are effects of resolution in the middle panels of Fig. 6, these effects, namely the differences between the middle and upper panels in the Figure, are almost too small to be visible. This means that the effects of resolution seen in the jet shapes in Fig. 5, which were already small in magnitude, are reduced further by cancellation when we look at differences between leading and subleading jets as in the definition of the  $\langle \not{p}_T^\parallel \rangle$  observable.

The particular discrepancy between the top and bottom panels of Fig. 6, which is to say between the predictions of the hybrid model and experimental measurements, that was highlighted in Ref. [113] can be seen most clearly by looking at the orange histograms, namely the contributions of hadrons with  $2 \text{ GeV} < p_T < 4 \text{ GeV}$ . In the hybrid model, the orange contribution to  $\langle \not{p}_T^\parallel \rangle$  is negative, meaning that in this  $p_T$ -range the greater energy loss of the subleading jet is more important than the larger wake of the subleading jet — in the model. In the experimental data in the bottom panels, the orange contribution to  $\langle \not{p}_T^\parallel \rangle$  is positive, meaning that in reality the larger wake of the subleading jet dominates in this  $p_T$ -range. This means that in the experimental data there are more hadrons coming from the wake with  $p_T$  in this range than in the hybrid model. Correspondingly, if we look at hadrons with  $p_T < 2 \text{ GeV}$ , the blue and yellow histograms, we see that there are fewer hadrons coming from the wake with  $p_T$  in this softest range in experimental data than in the hybrid model. We now see, from the middle panels of Fig. 6, that including the effects of resolution does not significantly ameliorate these discrepancies. This provides us with indirect evidence that these discrepancies are indeed telling us about the inadequacies of our treatment of the wake and, in particular, are telling us that the wakes that the jets leave in the plasma do not fully equilibrate, meaning that the hadrons that come from these wakes are not as soft in reality as in our fully equilibrated analysis.

A different way to present the physics contained in Fig. 6 is to present the  $\langle \not{p}_T^\parallel \rangle$  distributions integrated in  $\Delta$ , but sliced instead in terms of the dijet asymmetry variable  $A_J$ , defined as  $A_J \equiv (p_T^{\text{leading}} - p_T^{\text{subleading}})/(p_T^{\text{leading}} + p_T^{\text{subleading}})$ . This is done in Fig. 7, for two different centrality classes in the left and right columns. We only show dijets reconstructed with anti- $k_t$   $R = 0.3$ . The top two rows of panels show the results of our simulations (with  $L_{\text{res}} = 0$  and  $L_{\text{res}} = 2/\pi T$ ) and the bottom panels show CMS data [39]. Here again, the differences between the middle and upper panels, namely the effects of resolution, are almost too small to be visible. And, here again these effects do not explain the discrepancies between the hybrid model predictions in orange, as well as

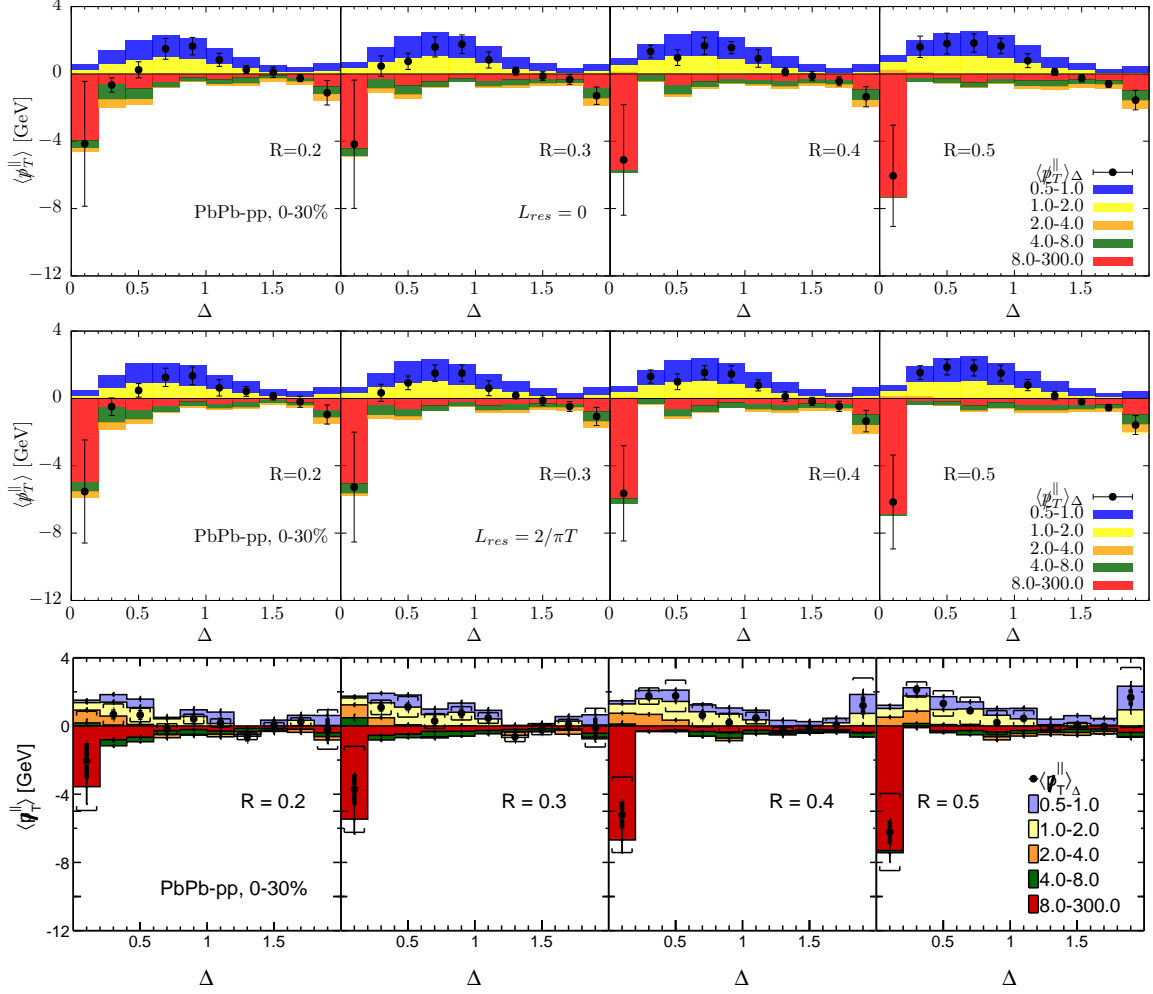


**Figure 6:** The observable  $\langle \not{p}_T^{\parallel} \rangle$ , defined as the average of  $\not{p}_T^{\parallel}$  in (5.2) over tracks, characterizes the momentum flow along the dijet direction with momentum pointing in the hemisphere of the leading/subleading jet counting negatively/positively and is referred to as the “missing- $p_T$ .” Here, we plot the difference of the missing- $p_T$  in Pb-Pb and p-p collisions. The upper row of panels shows the predictions of the hybrid model with  $L_{res} = 0$  from Ref. [113] for dijets reconstructed with four different values of the anti- $k_t$  reconstruction parameter,  $R$ . The colored histograms represent the contributions to the missing- $p_T$  coming from hadrons in specified  $p_T$  ranges, as a function of the angle relative to the dijet direction,  $\Delta$ ; the points with error bars show the sum of the missing- $p_T$  for hadrons with any  $p_T$ . The lower row of panels shows experimental measurements of this observable from the CMS collaboration [39]. The middle row of panels shows our results, obtained from the hybrid model with  $L_{res} = 2/\pi T$ . There are effects of resolution, namely differences between the middle and upper panels, but they are almost too small to be seen on the scale at which the plot is made, meaning that they are substantially smaller than the discrepancies between the hybrid model predictions in the upper panels and the experimental results in the lower panels.

in blue plus yellow, and the experimental measurements.

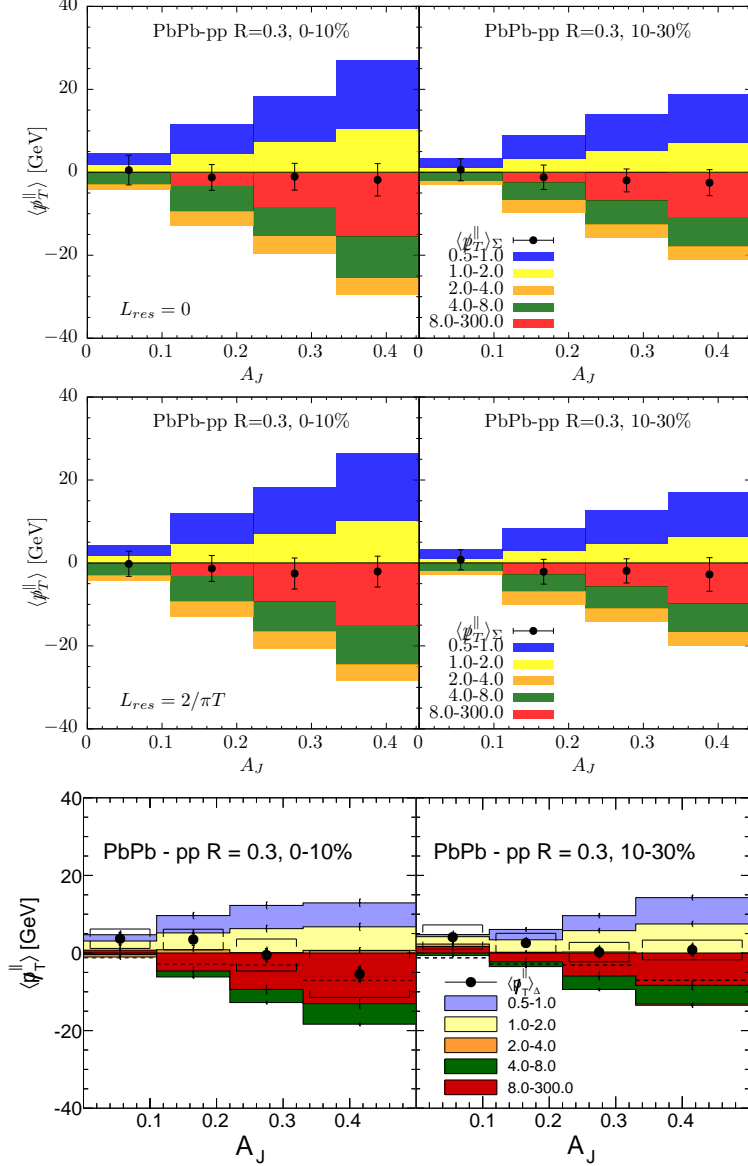


**Figure 7:** This missing- $p_T$  observable characterizes the asymmetry between the spectrum of the leading and subleading jets, as in Fig. 6, but this time integrated in  $\Delta$  and sliced in terms of the dijet asymmetry variable,  $A_J$ . The contributions of hadrons in different  $p_T$ -ranges to  $\langle p_T^{\parallel} \rangle$  are color coded as before. There are effects of resolution, namely differences between the middle and upper panels. However, as in Fig. 6 they are almost too small to be seen, meaning that they are substantially smaller than the discrepancies between the hybrid model predictions and the experimental results from Ref. [39] shown in the lower panels.

## 6 Discussion and Outlook

In this paper, we have investigated the phenomenological implications for various jet quenching observables of the fact that the strongly coupled QGP produced in heavy ion collisions cannot resolve two partons in a jet shower when they are closer together than some resolution length  $L_{res}$ . Our study is exploratory in character, in three ways. First, it is built upon the hybrid strong/weak



coupling model for jet quenching, which combines a weakly coupled treatment of jet production and showering from PYTHIA with a treatment of parton energy loss that is patterned on the rate of energy loss obtained via a holographic calculation in a different strongly coupled gauge theory, as we described in Section 2. This model has been used successfully to describe various data sets and gain various insights, but it *is* only a model, limited by its ingredients. In many ways, the most interesting uses of a model like this are to find the instances where it fails to agree with experimental data, as this teaches us much more than simply constraining the parameters of the model can. The analysis of this paper provides an example. Second, we assume that  $L_{\text{res}}$  is of order the Debye length and hence choose  $L_{\text{res}} = R_{\text{res}}/\pi T$  with  $R_{\text{res}}$  a constant that we treat as a new parameter of the model. As we described in Section 3, this is reasonable for a strongly coupled plasma and in some, but not all, kinematical regimes in a weakly coupled plasma. We saw that in some kinematical regimes at weak coupling,  $L_{\text{res}}$  could be shorter than the Debye length which would reduce the observable effects of resolution relative to what we have found. We looked at results for  $R_{\text{res}} = 1$  and 2, motivated by strong and weak coupling calculations of the Debye length, as well as for  $R_{\text{res}} = 5$ , which is a larger value than is physically motivated. Third, even though it is inescapable that the plasma has some nonzero resolution length  $L_{\text{res}}$  and so must perceive the jet shower in terms of a collection of effective partons, our implementation of the effects of resolution is simplified considerably, as we described in Section 4. When a parent parton splits into two offspring, we treat the offspring as a single effective parton with the energy, energy loss, and trajectory of the parent until the offspring are separated by more than  $L_{\text{res}}$  in the laboratory frame, and at that instant in time in the laboratory frame we replace the single effective parton by the two offspring which henceforth begin to lose energy independently. The need to specify a frame, together with certain other aspects of the way in which we build effective partons that we describe in Section 4, has a certain arbitrariness to it because we are not treating the (quantum mechanical) processes via which resolution occurs in full. The virtue of our implementation is that it constitutes a simple and unambiguous prescription that allows us to assess the magnitude of the effects of resolution on various jet and intra-jet observables upon exploring a set of reasonable values for the resolution length,  $L_{\text{res}}$ . All three of these exploratory aspects of our study could be revisited in future work, although the motivation for such efforts is reduced given that we find that including a reasonable nonzero value for  $L_{\text{res}}$  results in only modest changes to the model predictions for the observables that we have investigated.

As we increase  $L_{\text{res}}$ , the number of effective sources of energy loss is reduced since it takes longer for the medium to resolve the partons formed after each splitting. We saw in Section 5.1 that this increases the number of final state partons with moderate energies whose energy loss is the same as the average energy loss of the jet as a whole, not more. We saw in Section 5.2 that this results in a reduction in the total energy lost by the jet, which gets compensated for by an increase in  $\kappa_{\text{sc}}$ , the hybrid model parameter that controls the magnitude of the rate of energy loss for all partons in the jet, in order to maintain the agreement between the prediction of the model for jet  $R_{AA}$  and the experimentally measured value of this quantity. Consequently, when we turn on  $L_{\text{res}}$  we end up with jets within which the few hardest hadrons at the core of the jet lose modestly more energy and within which hadrons with moderate energies lose modestly less energy, making them more likely to survive and populate the jet at larger angles relative to its core. We illustrated both effects by computing model predictions for fragmentation functions and for the jet shape observable in

Section 5.3, showing that both depend on  $L_{\text{res}}$  in the expected fashion. We defer the study of single hadron  $R_{AA}$  and its potential sensitivity to  $L_{\text{res}}$  to future work, but note here that turning on  $L_{\text{res}}$  should push it somewhat downward since it is controlled by the hardest parton in each jet.

As we noted in Section 5.3, including the effects of resolution pushes the predictions of the hybrid model for fragmentation functions and jet shapes toward their experimentally measured values, but the effects are modest in magnitude and the discrepancies between the predictions of the model and the data that were highlighted in Ref. [113] remain. This provides indirect support for the alternative suggestion for the origin of these discrepancies, namely that they are telling us that the treatment of the backreaction of the plasma to the jets that we have implemented, following Ref. [113], is not sufficient in detail. In Ref. [113], this hypothesis was investigated further via computing the hybrid model predictions for several missing- $p_T$  observables, comparing them to experimental data, and finding significant discrepancies, in particular for hadrons with  $2 \text{ GeV} < p_T < 4 \text{ GeV}$ . In Section 5.4 we carried out this computation with  $L_{\text{res}}$  turned on, and found that the model predictions for these missing- $p_T$  observables with  $L_{\text{res}}$  set to  $2/\pi T$  are very similar to those with  $L_{\text{res}} = 0$ , with the differences almost too small to see relative to the interesting remaining discrepancies between the model predictions and data. This provides direct support for the conclusion that these discrepancies are not due to the effects of resolution and indirect support for the suggestion that they are telling us that the wakes left in the plasma by passing jets do not have time to equilibrate fully, since if they had done so the wakes would have yielded more hadrons with  $p_T < 2 \text{ GeV}$  and fewer hadrons with  $2 \text{ GeV} < p_T < 4 \text{ GeV}$  reconstructed within the jets, as in the model calculation. This result motivates a full event-by-event hydrodynamic treatment of the wakes that goes beyond the linear approximations that we have employed and suggests that a comparison between the predictions of such a treatment and data could provide a snapshot of a non-equilibrium disturbance of the strongly coupled plasma as it is equilibrating, but not yet equilibrated. These conclusions confirm the importance of further measurements of experimental observables that are sensitive to the distribution of partons within the jet shower as a function of energy and angle, which have increasing statistical precision, which are increasingly differential, and which employ jets produced back-to-back with photons or  $Z$ -bosons as well as in dijet pairs.

## Acknowledgments

We thank J. Casalderrey-Solana, D. Gulhan, G. Milhano, and K. Zapp for helpful discussions. We also thank J. Balewski, M. Goncharov, and C. Paus for their assistance with computing. ZH and KR acknowledge the hospitality of the CERN Theory Group. DP acknowledges the hospitality of the MIT Center for Theoretical Physics. The work of ZH was supported by the Undergraduate Research Opportunity Program at MIT. The work of DP was supported by the U.S. National Science Foundation within the framework of the JETSCAPE collaboration, under grant number ACI-1550300, and also by grants FPA2013-46570 and MDM-2014-0369 of ICCUB (Unidad de Excelencia ‘María de Maeztu’) from the Spanish MINECO, by grant 2014-SGR-104 from the Generalitat de Catalunya, and by the Consolider CPAN project. The work of KR was supported by the U.S. Department of Energy under grant Contract Number DE-SC0011090.

## References

- [1] K. Adcox *et al.* [PHENIX Collaboration], “Formation of dense partonic matter in relativistic nucleus-nucleus collisions at RHIC: Experimental evaluation by the PHENIX collaboration,” Nucl. Phys. A **757**, 184 (2005) [nucl-ex/0410003].
- [2] I. Arsene *et al.* [BRAHMS Collaboration], “Quark gluon plasma and color glass condensate at RHIC? The Perspective from the BRAHMS experiment,” Nucl. Phys. A **757**, 1 (2005) [nucl-ex/0410020].
- [3] B. B. Back *et al.*, “The PHOBOS perspective on discoveries at RHIC,” Nucl. Phys. A **757**, 28 (2005) [nucl-ex/0410022].
- [4] J. Adams *et al.* [STAR Collaboration], “Experimental and theoretical challenges in the search for the quark gluon plasma: The STAR Collaboration’s critical assessment of the evidence from RHIC collisions,” Nucl. Phys. A **757**, 102 (2005) [nucl-ex/0501009].
- [5] K. Aamodt *et al.* [ALICE Collaboration], “Elliptic flow of charged particles in Pb-Pb collisions at 2.76 TeV,” Phys. Rev. Lett. **105**, 252302 (2010) doi:10.1103/PhysRevLett.105.252302 [arXiv:1011.3914 [nucl-ex]].
- [6] G. Aad *et al.* [ATLAS Collaboration], “Measurement of the pseudorapidity and transverse momentum dependence of the elliptic flow of charged particles in lead-lead collisions at  $\sqrt{s_{NN}} = 2.76$  TeV with the ATLAS detector,” Phys. Lett. B **707**, 330 (2012) [arXiv:1108.6018 [hep-ex]].
- [7] S. Chatrchyan *et al.* [CMS Collaboration], “Measurement of the elliptic anisotropy of charged particles produced in PbPb collisions at  $\sqrt{s_{NN}}=2.76$  TeV,” Phys. Rev. C **87**, no. 1, 014902 (2013) [arXiv:1204.1409 [nucl-ex]].
- [8] P. Huovinen, P. F. Kolb, U. W. Heinz, P. V. Ruuskanen and S. A. Voloshin, “Radial and elliptic flow at RHIC: Further predictions,” Phys. Lett. B **503**, 58 (2001) [hep-ph/0101136].
- [9] D. Teaney, J. Lauret and E. V. Shuryak, “A Hydrodynamic description of heavy ion collisions at the SPS and RHIC,” nucl-th/0110037.
- [10] T. Hirano, U. W. Heinz, D. Kharzeev, R. Lacey and Y. Nara, “Hadronic dissipative effects on elliptic flow in ultrarelativistic heavy-ion collisions,” Phys. Lett. B **636**, 299 (2006) [nucl-th/0511046].
- [11] P. Romatschke and U. Romatschke, “Viscosity Information from Relativistic Nuclear Collisions: How Perfect is the Fluid Observed at RHIC?,” Phys. Rev. Lett. **99**, 172301 (2007) [arXiv:0706.1522 [nucl-th]].
- [12] M. Luzum and P. Romatschke, “Conformal Relativistic Viscous Hydrodynamics: Applications to RHIC results at  $\sqrt{s_{NN}} = 200$  GeV,” Phys. Rev. C **78**, 034915 (2008); Erratum: [Phys. Rev. C **79**, 039903 (2009)] [arXiv:0804.4015 [nucl-th]].
- [13] B. Schenke, S. Jeon and C. Gale, “Elliptic and triangular flow in event-by-event (3+1)D viscous hydrodynamics,” Phys. Rev. Lett. **106**, 042301 (2011) [arXiv:1009.3244 [hep-ph]].
- [14] T. Hirano, P. Huovinen and Y. Nara, “Elliptic flow in Pb+Pb collisions at  $\sqrt{s_{NN}} = 2.76$  TeV: hybrid model assessment of the first data,” Phys. Rev. C **84**, 011901 (2011) [arXiv:1012.3955 [nucl-th]].
- [15] C. Gale, S. Jeon, B. Schenke, P. Tribedy and R. Venugopalan, “Event-by-event anisotropic flow in heavy-ion collisions from combined Yang-Mills and viscous fluid dynamics,” Phys. Rev. Lett. **110**, no. 1, 012302 (2013) [arXiv:1209.6330 [nucl-th]].
- [16] C. Shen, Z. Qiu, H. Song, J. Bernhard, S. Bass and U. Heinz, “The iEBE-VISHNU code package for relativistic heavy-ion collisions,” arXiv:1409.8164 [nucl-th].

- [17] C. Shen, J. F. Paquet, U. Heinz and C. Gale, “Photon Emission from a Momentum Anisotropic Quark-Gluon Plasma,” *Phys. Rev. C* **91**, no. 1, 014908 (2015) [arXiv:1410.3404 [nucl-th]].
- [18] J. E. Bernhard, J. S. Moreland, S. A. Bass, J. Liu and U. Heinz, “Applying Bayesian parameter estimation to relativistic heavy-ion collisions: simultaneous characterization of the initial state and quark-gluon plasma medium,” arXiv:1605.03954 [nucl-th].
- [19] G. Policastro, D. T. Son and A. O. Starinets, “The Shear viscosity of strongly coupled  $\mathcal{N} = 4$  supersymmetric Yang-Mills plasma,” *Phys. Rev. Lett.* **87**, 081601 (2001) [hep-th/0104066].
- [20] A. Buchel and J. T. Liu, “Universality of the shear viscosity in supergravity,” *Phys. Rev. Lett.* **93**, 090602 (2004) [hep-th/0311175].
- [21] P. Kovtun, D. T. Son and A. O. Starinets, “Viscosity in strongly interacting quantum field theories from black hole physics,” *Phys. Rev. Lett.* **94**, 111601 (2005) [hep-th/0405231].
- [22] G. Aad *et al.* [ATLAS Collaboration], “Observation of a Centrality-Dependent Dijet Asymmetry in Lead-Lead Collisions at  $\sqrt{s_{NN}} = 2.77$  TeV with the ATLAS Detector at the LHC,” *Phys. Rev. Lett.* **105**, 252303 (2010) [arXiv:1011.6182 [hep-ex]].
- [23] S. Chatrchyan *et al.* [CMS Collaboration], “Observation and studies of jet quenching in PbPb collisions at nucleon-nucleon center-of-mass energy = 2.76 TeV,” *Phys. Rev. C* **84**, 024906 (2011) [arXiv:1102.1957 [nucl-ex]].
- [24] S. Chatrchyan *et al.* [CMS Collaboration], “Jet momentum dependence of jet quenching in PbPb collisions at  $\sqrt{s_{NN}} = 2.76$  TeV,” *Phys. Lett. B* **712**, 176 (2012) [arXiv:1202.5022 [nucl-ex]].
- [25] S. Chatrchyan *et al.* [CMS Collaboration], “Studies of jet quenching using isolated-photon+jet correlations in PbPb and pp collisions at  $\sqrt{s_{NN}} = 2.76$  TeV,” *Phys. Lett. B* **718**, 773 (2013) [arXiv:1205.0206 [nucl-ex]].
- [26] S. Chatrchyan *et al.* [CMS Collaboration], “Measurement of jet fragmentation into charged particles in pp and PbPb collisions at  $\sqrt{s_{NN}} = 2.76$  TeV,” *JHEP* **1210**, 087 (2012) [arXiv:1205.5872 [nucl-ex]].
- [27] G. Aad *et al.* [ATLAS Collaboration], “Measurement of the jet radius and transverse momentum dependence of inclusive jet suppression in lead-lead collisions at  $\sqrt{s_{NN}} = 2.76$  TeV with the ATLAS detector,” *Phys. Lett. B* **719**, 220 (2013) [arXiv:1208.1967 [hep-ex]].
- [28] CMS Collaboration, “Nuclear modification factor of high transverse momentum jets in PbPb collisions at  $\sqrt{s_{NN}} = 2.76$  TeV”, CMS PAS HIN-12-004.
- [29] G. Aad *et al.* [ATLAS Collaboration], “Measurement of the Azimuthal Angle Dependence of Inclusive Jet Yields in Pb+Pb Collisions at  $\sqrt{s_{NN}} = 2.76$  TeV with the ATLAS detector,” *Phys. Rev. Lett.* **111**, no. 15, 152301 (2013) [arXiv:1306.6469 [hep-ex]].
- [30] S. Chatrchyan *et al.* [CMS Collaboration], “Modification of jet shapes in PbPb collisions at  $\sqrt{s_{NN}} = 2.76$  TeV,” *Phys. Lett. B* **730**, 243 (2014) [arXiv:1310.0878 [nucl-ex]].
- [31] B. Abelev *et al.* [ALICE Collaboration], “Measurement of charged jet suppression in Pb-Pb collisions at  $\sqrt{s_{NN}} = 2.76$  TeV,” *JHEP* **1403**, 013 (2014) [arXiv:1311.0633 [nucl-ex]].
- [32] S. Chatrchyan *et al.* [CMS Collaboration], “Evidence of b-Jet Quenching in PbPb Collisions at  $\sqrt{s_{NN}} = 2.76$  TeV,” *Phys. Rev. Lett.* **113**, no. 13, 132301 (2014) [*Phys. Rev. Lett.* **115**, no. 2, 029903 (2015)] [arXiv:1312.4198 [nucl-ex]].
- [33] S. Chatrchyan *et al.* [CMS Collaboration], “Measurement of jet fragmentation in PbPb and pp collisions at  $\sqrt{s_{NN}} = 2.76$  TeV,” *Phys. Rev. C* **90**, no. 2, 024908 (2014) [arXiv:1406.0932 [nucl-ex]].

- [34] G. Aad *et al.* [ATLAS Collaboration], “Measurement of inclusive jet charged-particle fragmentation functions in Pb+Pb collisions at  $\sqrt{s_{NN}} = 2.76$  TeV with the ATLAS detector,” *Phys. Lett. B* **739**, 320 (2014) [arXiv:1406.2979 [hep-ex]].
- [35] G. Aad *et al.* [ATLAS Collaboration], “Measurements of the Nuclear Modification Factor for Jets in Pb+Pb Collisions at  $\sqrt{s_{NN}} = 2.76$  TeV with the ATLAS Detector,” *Phys. Rev. Lett.* **114**, no. 7, 072302 (2015) [arXiv:1411.2357 [hep-ex]].
- [36] J. Adam *et al.* [ALICE Collaboration], “Measurement of jet suppression in central Pb-Pb collisions at  $\sqrt{s_{NN}} = 2.76$  TeV,” *Phys. Lett. B* **746**, 1 (2015) [arXiv:1502.01689 [nucl-ex]].
- [37] J. Adam *et al.* [ALICE Collaboration], “Measurement of jet quenching with semi-inclusive hadron-jet distributions in central Pb-Pb collisions at  $\sqrt{s_{NN}} = 2.76$  TeV,” arXiv:1506.03984 [nucl-ex].
- [38] G. Aad *et al.* [ATLAS Collaboration], “Measurement of the production of neighbouring jets in lead-lead collisions at  $\sqrt{s_{NN}} = 2.76$  TeV with the ATLAS detector,” arXiv:1506.08656 [hep-ex].
- [39] V. Khachatryan *et al.* [CMS Collaboration], “Measurement of transverse momentum relative to dijet systems in PbPb and pp collisions at  $\sqrt{s_{NN}} = 2.76$  TeV,” *JHEP* **1601**, 006 (2016) [arXiv:1509.09029 [nucl-ex]].
- [40] V. Khachatryan *et al.* [CMS Collaboration], “Correlations between jets and charged particles in PbPb and pp collisions at  $\sqrt{s_{NN}} = 2.76$  TeV,” *JHEP* **1602**, 156 (2016) [arXiv:1601.00079 [nucl-ex]].
- [41] V. Khachatryan *et al.* [CMS Collaboration], “Study of Isolated-Photon + Jet Correlations in PbPb and pp Collisions at  $\sqrt{s_{NN}} = 5.02$  TeV” CMS PAS HIN-16-002 (2016).
- [42] V. Khachatryan *et al.* [CMS Collaboration], “Decomposing transverse momentum balance contributions for quenched jets in PbPb collisions at  $\sqrt{s_{NN}} = 2.76$  TeV,” *JHEP* **1611**, 055 (2016) [arXiv:1609.02466 [nucl-ex]].
- [43] V. Khachatryan *et al.* [CMS Collaboration], “Measurement of inclusive jet cross-sections in pp and PbPb collisions at  $\sqrt{s_{NN}}=2.76$  TeV,” Submitted to: *Phys.Rev.C* [arXiv:1609.05383 [nucl-ex]].
- [44] M. Aaboud *et al.* [ATLAS Collaboration], “Measurement of jet fragmentation in Pb+Pb and pp collisions at  $\sqrt{s_{NN}} = 2.76$  TeV with the ATLAS detector at the LHC,” *Eur. Phys. J. C* **77**, no. 6, 379 (2017) [arXiv:1702.00674 [hep-ex]].
- [45] S. Acharya *et al.* [ALICE Collaboration], “First measurement of jet mass in Pb-Pb and p-Pb collisions at the LHC,” arXiv:1702.00804 [nucl-ex].
- [46] A. M. Sirunyan *et al.* [CMS Collaboration], “Study of jet quenching with Z+jet correlations in PbPb and pp collisions at  $\sqrt{s_{NN}} = 5.02$  TeV,” arXiv:1702.01060 [nucl-ex].
- [47] M. Aaboud *et al.* [ATLAS Collaboration], “Measurement of jet  $p_T$  correlations in Pb+Pb and pp collisions at  $\sqrt{s_{NN}} = 2.76$  TeV with the ATLAS detector,” arXiv:1706.09363 [hep-ex].
- [48] K. Adcox *et al.* [PHENIX Collaboration], “Suppression of hadrons with large transverse momentum in central Au+Au collisions at  $\sqrt{s_{NN}} = 130$  GeV,” *Phys. Rev. Lett.* **88**, 022301 (2002) [nucl-ex/0109003].
- [49] C. Adler *et al.* [STAR Collaboration], “Centrality dependence of high  $p_T$  hadron suppression in Au+Au collisions at  $\sqrt{s_{NN}} = 130$  GeV,” *Phys. Rev. Lett.* **89**, 202301 (2002) [nucl-ex/0206011].
- [50] C. Adler *et al.* [STAR Collaboration], “Disappearance of back-to-back high  $p_T$  hadron correlations in central Au+Au collisions at  $\sqrt{s_{NN}} = 200$ -GeV,” *Phys. Rev. Lett.* **90**, 082302 (2003) [nucl-ex/0210033].

- [51] M. Ploskon [STAR Collaboration], “Inclusive cross section and correlations of fully reconstructed jets in  $\sqrt{s_{NN}} = 200$  GeV Au+Au and p+p collisions,” Nucl. Phys. A **830**, 255C (2009) [arXiv:0908.1799 [nucl-ex]].
- [52] D. V. Perepelitsa [PHENIX Collaboration], “Reconstructed Jet Results in p + p, d + Au and Cu + Cu collisions at 200 GeV from PHENIX,” Nucl. Phys. A **910-911**, 425 (2013).
- [53] L. Adamczyk *et al.* [STAR Collaboration], “Jet-Hadron Correlations in  $\sqrt{s_{NN}} = 200$  GeV p+p and Central Au+Au Collisions,” Phys. Rev. Lett. **112**, no. 12, 122301 (2014) [arXiv:1302.6184 [nucl-ex]].
- [54] P. M. Jacobs *et al.* [STAR Collaboration], “Measurements of jet quenching with semi-inclusive charged jet distributions in Au + Au collisions at  $\sqrt{s_{NN}} = 200$  GeV,” arXiv:1512.08784 [nucl-ex].
- [55] L. Adamczyk *et al.* [STAR Collaboration], “Di-Jet Imbalance Measurements at  $\sqrt{s_{NN}} = 200$  GeV at STAR,” arXiv:1609.03878 [nucl-ex].
- [56] L. Adamczyk *et al.* [STAR Collaboration], “Measurements of jet quenching with semi-inclusive hadron+jet distributions in Au+Au collisions at  $\sqrt{s_{NN}} = 200$  GeV,” arXiv:1702.01108 [nucl-ex].
- [57] A. Adare *et al.*, “An Upgrade Proposal from the PHENIX Collaboration,” arXiv:1501.06197 [nucl-ex].
- [58] P. Jacobs and X. N. Wang, “Matter in extremis: Ultrarelativistic nuclear collisions at RHIC,” Prog. Part. Nucl. Phys. **54**, 443 (2005) [arXiv:hep-ph/0405125].
- [59] J. Casalderrey-Solana, C. A. Salgado, “Introductory lectures on jet quenching in heavy ion collisions,” Acta Phys. Polon. **B38**, 3731-3794 (2007). [arXiv:0712.3443 [hep-ph]].
- [60] A. Majumder, M. Van Leeuwen, “The theory and phenomenology of perturbative QCD based jet quenching,” [arXiv:1002.2206 [hep-ph]].
- [61] J. Ghiglieri and D. Teaney, “Parton energy loss and momentum broadening at NLO in high temperature QCD plasmas,” Int. J. Mod. Phys. E **24**, no. 11, 1530013 (2015) [arXiv:1502.03730 [hep-ph]].
- [62] J. P. Blaizot and Y. Mehtar-Tani, “Jet Structure in Heavy Ion Collisions,” Int. J. Mod. Phys. E **24**, no. 11, 1530012 (2015) [arXiv:1503.05958 [hep-ph]].
- [63] G. Y. Qin and X. N. Wang, “Jet quenching in high-energy heavy-ion collisions,” Int. J. Mod. Phys. E **24**, no. 11, 1530014 (2015) [arXiv:1511.00790 [hep-ph]].
- [64] K. Zapp, J. Stachel and U. A. Wiedemann, “A Local Monte Carlo implementation of the non-abelian Landau-Pomeranchuk-Migdal effect,” Phys. Rev. Lett. **103**, 152302 (2009) [arXiv:0812.3888 [hep-ph]].
- [65] K. Zapp, G. Ingelman, J. Rathsman, J. Stachel and U. A. Wiedemann, “A Monte Carlo Model for ‘Jet Quenching’,” Eur. Phys. J. C **60**, 617 (2009) [arXiv:0804.3568 [hep-ph]].
- [66] N. Armesto, L. Cunqueiro and C. A. Salgado, “Q-PYTHIA: A Medium-modified implementation of final state radiation,” Eur. Phys. J. C **63**, 679 (2009) [arXiv:0907.1014 [hep-ph]].
- [67] B. Schenke, C. Gale and S. Jeon, “MARTINI: An Event generator for relativistic heavy-ion collisions,” Phys. Rev. C **80**, 054913 (2009) [arXiv:0909.2037 [hep-ph]].
- [68] I. P. Lokhtin, A. V. Belyaev and A. M. Snigirev, “Jet quenching pattern at LHC in PYQUEN model,” Eur. Phys. J. C **71**, 1650 (2011) [arXiv:1103.1853 [hep-ph]].
- [69] K. C. Zapp, F. Krauss and U. A. Wiedemann, “A perturbative framework for jet quenching,” JHEP **1303**, 080 (2013) [arXiv:1212.1599 [hep-ph]].

- [70] K. C. Zapp, “JEWEL 2.0.0: directions for use,” *Eur. Phys. J. C* **74**, no. 2, 2762 (2014) [arXiv:1311.0048 [hep-ph]].
- [71] K. C. Zapp, “Geometrical aspects of jet quenching in JEWEL,” *Phys. Lett. B* **735**, 157 (2014) [arXiv:1312.5536 [hep-ph]].
- [72] J. M. Maldacena, “The Large N limit of superconformal field theories and supergravity,” *Int. J. Theor. Phys.* **38**, 1113 (1999) [*Adv. Theor. Math. Phys.* **2**, 231 (1998)] [hep-th/9711200].
- [73] J. Casalderrey-Solana, H. Liu, D. Mateos, K. Rajagopal and U. A. Wiedemann, “Gauge/String Duality, Hot QCD and Heavy Ion Collisions,” Cambridge University Press, 2014; see also arXiv:1101.0618 [hep-th].
- [74] O. DeWolfe, S. S. Gubser, C. Rosen and D. Teaney, “Heavy ions and string theory,” *Prog. Part. Nucl. Phys.* **75**, 86 (2014) [arXiv:1304.7794 [hep-th]].
- [75] P. M. Chesler and W. van der Schee, “Early thermalization, hydrodynamics and energy loss in AdS/CFT,” *Int. J. Mod. Phys. E* **24**, no. 10, 1530011 (2015) [arXiv:1501.04952 [nucl-th]].
- [76] C. P. Herzog, A. Karch, P. Kovtun, C. Kozcaz and L. G. Yaffe, “Energy loss of a heavy quark moving through  $\mathcal{N} = 4$  supersymmetric Yang-Mills plasma,” *JHEP* **0607**, 013 (2006) [hep-th/0605158].
- [77] H. Liu, K. Rajagopal and U. A. Wiedemann, “Calculating the jet quenching parameter from AdS/CFT,” *Phys. Rev. Lett.* **97**, 182301 (2006) [hep-ph/0605178].
- [78] J. Casalderrey-Solana and D. Teaney, “Heavy quark diffusion in strongly coupled  $\mathcal{N} = 4$  Yang-Mills,” *Phys. Rev. D* **74**, 085012 (2006) [hep-ph/0605199].
- [79] S. S. Gubser, “Drag force in AdS/CFT,” *Phys. Rev. D* **74**, 126005 (2006) [hep-th/0605182].
- [80] H. Liu, K. Rajagopal and U. A. Wiedemann, “An AdS/CFT Calculation of Screening in a Hot Wind,” *Phys. Rev. Lett.* **98**, 182301 (2007) [hep-ph/0607062].
- [81] M. Chernicoff, J. A. Garcia and A. Guijosa, “The Energy of a Moving Quark-Antiquark Pair in an  $\mathcal{N} = 4$  SYM Plasma,” *JHEP* **0609**, 068 (2006) [hep-th/0607089].
- [82] H. Liu, K. Rajagopal and U. A. Wiedemann, “Wilson loops in heavy ion collisions and their calculation in AdS/CFT,” *JHEP* **0703**, 066 (2007) [hep-ph/0612168].
- [83] S. S. Gubser, “Momentum fluctuations of heavy quarks in the gauge-string duality,” *Nucl. Phys. B* **790**, 175 (2008) [hep-th/0612143].
- [84] J. Casalderrey-Solana and D. Teaney, “Transverse Momentum Broadening of a Fast Quark in a  $\mathcal{N} = 4$  Yang Mills Plasma,” *JHEP* **0704**, 039 (2007) [hep-th/0701123].
- [85] P. M. Chesler and L. G. Yaffe, “The Wake of a quark moving through a strongly-coupled plasma,” *Phys. Rev. Lett.* **99**, 152001 (2007) [arXiv:0706.0368 [hep-th]].
- [86] S. S. Gubser, S. S. Pufu and A. Yarom, “Sonic booms and diffusion wakes generated by a heavy quark in thermal AdS/CFT,” *Phys. Rev. Lett.* **100**, 012301 (2008) [arXiv:0706.4307 [hep-th]].
- [87] P. M. Chesler and L. G. Yaffe, “The Stress-energy tensor of a quark moving through a strongly-coupled  $\mathcal{N}=4$  supersymmetric Yang-Mills plasma: Comparing hydrodynamics and AdS/CFT,” *Phys. Rev. D* **78**, 045013 (2008) [arXiv:0712.0050 [hep-th]].
- [88] D. M. Hofman and J. Maldacena, “Conformal collider physics: Energy and charge correlations,” *JHEP* **0805**, 012 (2008) [arXiv:0803.1467 [hep-th]].
- [89] S. S. Gubser, D. R. Gulotta, S. S. Pufu and F. D. Rocha, “Gluon energy loss in the gauge-string duality,” *JHEP* **0810**, 052 (2008) [arXiv:0803.1470 [hep-th]].

- [90] Y. Hatta, E. Iancu and A. H. Mueller, “Jet evolution in the  $\mathcal{N} = 4$  SYM plasma at strong coupling,” *JHEP* **0805**, 037 (2008) [arXiv:0803.2481 [hep-th]].
- [91] F. Dominguez, C. Marquet, A. H. Mueller, B. Wu and B. W. Xiao, “Comparing energy loss and perpendicular - broadening in perturbative QCD with strong coupling  $\mathcal{N} = 4$  SYM theory,” *Nucl. Phys. A* **811**, 197 (2008) [arXiv:0803.3234 [nucl-th]].
- [92] P. M. Chesler, K. Jensen and A. Karch, “Jets in strongly-coupled  $\mathcal{N} = 4$  super Yang-Mills theory,” *Phys. Rev. D* **79**, 025021 (2009) [arXiv:0804.3110 [hep-th]].
- [93] P. M. Chesler, K. Jensen, A. Karch and L. G. Yaffe, “Light quark energy loss in strongly-coupled  $\mathcal{N} = 4$  supersymmetric Yang-Mills plasma,” *Phys. Rev. D* **79**, 125015 (2009) [arXiv:0810.1985 [hep-th]].
- [94] F. D’Eramo, H. Liu and K. Rajagopal, “Transverse Momentum Broadening and the Jet Quenching Parameter, Redux,” *Phys. Rev. D* **84**, 065015 (2011) [arXiv:1006.1367 [hep-ph]].
- [95] P. Arnold and D. Vaman, “Jet quenching in hot strongly coupled gauge theories revisited: 3-point correlators with gauge-gravity duality,” *JHEP* **1010**, 099 (2010) [arXiv:1008.4023 [hep-th]].
- [96] P. Arnold and D. Vaman, “Jet quenching in hot strongly coupled gauge theories simplified,” *JHEP* **1104**, 027 (2011) [arXiv:1101.2689 [hep-th]].
- [97] P. Arnold and D. Vaman, “Some new results for ‘jet’ stopping in AdS/CFT: long version,” *J. Phys. G* **38**, 124175 (2011) [arXiv:1106.1680 [hep-th]].
- [98] M. Chernicoff, J. A. Garcia, A. Guijosa and J. F. Pedraza, “Holographic Lessons for Quark Dynamics,” *J. Phys. G* **39**, 054002 (2012) [arXiv:1111.0872 [hep-th]].
- [99] P. M. Chesler, Y. -Y. Ho and K. Rajagopal, “Shining a Gluon Beam Through Quark-Gluon Plasma,” *Phys. Rev. D* **85**, 126006 (2012) [arXiv:1111.1691 [hep-th]].
- [100] P. Arnold, P. Szepietowski and D. Vaman, “Coupling dependence of jet quenching in hot strongly-coupled gauge theories,” *JHEP* **1207**, 024 (2012) [arXiv:1203.6658 [hep-th]].
- [101] P. Arnold, P. Szepietowski, D. Vaman and G. Wong, “Tidal stretching of gravitons into classical strings: application to jet quenching with AdS/CFT,” *JHEP* **1302**, 130 (2013) [arXiv:1212.3321 [hep-th]].
- [102] P. M. Chesler, M. Lekaveckas and K. Rajagopal, “Heavy quark energy loss far from equilibrium in a strongly coupled collision,” *JHEP* **1310**, 013 (2013) [arXiv:1306.0564 [hep-ph]].
- [103] A. Ficnar and S. S. Gubser, “Finite momentum at string endpoints,” *Phys. Rev. D* **89**, 026002 (2014) [arXiv:1306.6648 [hep-th]].
- [104] A. Ficnar, S. S. Gubser and M. Gyulassy, “Shooting String Holography of Jet Quenching at RHIC and LHC,” *Phys. Lett. B* **738**, 464 (2014) [arXiv:1311.6160 [hep-ph]].
- [105] P. M. Chesler and K. Rajagopal, “Jet quenching in strongly coupled plasma,” *Phys. Rev. D* **90**, no. 2, 025033 (2014) [arXiv:1402.6756 [hep-th]].
- [106] R. Rougemont, A. Ficnar, S. Finazzo and J. Noronha, “Energy loss, equilibration, and thermodynamics of a baryon rich strongly coupled quark-gluon plasma,” arXiv:1507.06556 [hep-th].
- [107] P. M. Chesler and K. Rajagopal, “On the Evolution of Jet Energy and Opening Angle in Strongly Coupled Plasma,” arXiv:1511.07567 [hep-th].
- [108] J. Casalderrey-Solana and A. Ficnar, “Holographic Three-Jet Events in Strongly Coupled  $\mathcal{N}=4$  Yang-Mills Plasma,” arXiv:1512.00371 [hep-th].



- [109] K. Rajagopal, A. V. Sadofyev and W. van der Schee, “Evolution of the jet opening angle distribution in holographic plasma,” *Phys. Rev. Lett.* **116**, no. 21, 211603 (2016) [arXiv:1602.04187 [nucl-th]].
- [110] J. Brewer, K. Rajagopal, A. Sadofyev and W. van der Schee, “Holographic Jet Shapes and their Evolution in Strongly Coupled Plasma,” arXiv:1704.05455 [nucl-th].
- [111] J. Casalderrey-Solana, D. C. Gulhan, J. G. Milhano, D. Pablos and K. Rajagopal, “A Hybrid Strong/Weak Coupling Approach to Jet Quenching,” *JHEP* **1410**, 19 (2014); Erratum: [*JHEP* **1509**, 175 (2015)] [arXiv:1405.3864 [hep-ph]].
- [112] J. Casalderrey-Solana, D. C. Gulhan, J. G. Milhano, D. Pablos and K. Rajagopal, “Predictions for Boson-Jet Observables and Fragmentation Function Ratios from a Hybrid Strong/Weak Coupling Model for Jet Quenching,” *JHEP* **1603**, 053 (2016) [arXiv:1508.00815 [hep-ph]].
- [113] J. Casalderrey-Solana, D. Gulhan, G. Milhano, D. Pablos and K. Rajagopal, “Angular Structure of Jet Quenching Within a Hybrid Strong/Weak Coupling Model,” *JHEP* **1703**, 135 (2017) [arXiv:1609.05842 [hep-ph]].
- [114] Y. Mehtar-Tani, C. A. Salgado and K. Tywoniuk, “Anti-angular ordering of gluon radiation in QCD media,” *Phys. Rev. Lett.* **106**, 122002 (2011) [arXiv:1009.2965 [hep-ph]].
- [115] Y. Mehtar-Tani, C. A. Salgado and K. Tywoniuk, “Jets in QCD Media: From Color Coherence to Decoherence,” *Phys. Lett. B* **707**, 156 (2012) [arXiv:1102.4317 [hep-ph]].
- [116] J. Casalderrey-Solana and E. Iancu, “Interference effects in medium-induced gluon radiation,” *JHEP* **1108**, 015 (2011) [arXiv:1105.1760 [hep-ph]].
- [117] J. Casalderrey-Solana, Y. Mehtar-Tani, C. A. Salgado and K. Tywoniuk, “New picture of jet quenching dictated by color coherence,” *Phys. Lett. B* **725**, 357 (2013) [arXiv:1210.7765 [hep-ph]].
- [118] J. G. Milhano and K. C. Zapp, “Origins of the di-jet asymmetry in heavy ion collisions,” *Eur. Phys. J. C* **76**, no. 5, 288 (2016) [arXiv:1512.08107 [hep-ph]].
- [119] M. A. Escobedo and E. Iancu, “Event-by-event fluctuations in the medium-induced jet evolution,” *JHEP* **1605**, 008 (2016) [arXiv:1601.03629 [hep-ph]].
- [120] T. Sjostrand, S. Mrenna and P. Z. Skands, “A Brief Introduction to PYTHIA 8.1,” *Comput. Phys. Commun.* **178**, 852 (2008) [arXiv:0710.3820 [hep-ph]].
- [121] M. Cacciari, G. P. Salam and G. Soyez, “The Anti- $k_t$  jet clustering algorithm,” *JHEP* **0804**, 063 (2008) [arXiv:0802.1189 [hep-ph]].
- [122] M. Cacciari, G. P. Salam and G. Soyez, “FastJet User Manual,” *Eur. Phys. J. C* **72** (2012) 1896 [arXiv:1111.6097 [hep-ph]].
- [123] D. Bak, A. Karch and L. G. Yaffe, “Debye screening in strongly coupled N=4 supersymmetric Yang-Mills plasma,” *JHEP* **0708**, 049 (2007) [arXiv:0705.0994 [hep-th]].
- [124] J. Casalderrey-Solana, D. Pablos and K. Tywoniuk, *JHEP* **1611**, 174 (2016) doi:10.1007/JHEP11(2016)174 [arXiv:1512.07561 [hep-ph]].
- [125] R. Baier, Y. L. Dokshitzer, A. H. Mueller, S. Peigne and D. Schiff, “Radiative energy loss and  $p_T$  broadening of high-energy partons in nuclei,” *Nucl. Phys. B* **484**, 265 (1997) [hep-ph/9608322].
- [126] F. D’Eramo, M. Lekaveckas, H. Liu and K. Rajagopal, “Momentum Broadening in Weakly Coupled Quark-Gluon Plasma (with a view to finding the quasiparticles within liquid quark-gluon plasma),” *JHEP* **1305**, 031 (2013) [arXiv:1211.1922 [hep-ph]].